Revista Internacional de Métodos Numéricos para Cálculo y Diseño en Ingeniería

Computational Analysis of Newly Topp-Leone Data Using Adaptive Progressive Type-II Censoring and Its Applications in Medical and Industrial Sciences

Heba S. Mohammed[1], **Osama E. Abo-Kasem**[2,*] **and Ahmed Elshahhat**[3]

[1]Department of Mathematical Sciences, College of Science, Princess Nourah bint Abdulrahman University, P.O. Box 84428, Riyadh, 11671, Saudi Arabia

[2]Department of Statistics, Faculty of Commerce, Zagazig University, Zagazig, 44519, Egypt

[3]Faculty of Technology and Development, Zagazig University, Zagazig, 44519, Egypt

ABSTRACT

Reliability analysis is critical in various scientific fields, necessitating robust lifetime models that effectively capture real-world failure mechanisms. This work explores a novel extension of the classical Topp-Leone (TL) lifespan model, called the generalized-TL (GTL) distribution, when datasets are gathered from adaptive progressive Type-II censoring. This model is highly superior for analyzing complex lifetime data with diverse hazard rate structures, including decreasing, increasing, and bathtub-shaped patterns. Employing both likelihood and Bayes estimation approaches, this work attempts to infer the unknown parameters and the reliability and failure rate functions of the GTL model. The Bayesian inference is created using the squared-error loss and independent gamma assumptions. Asymptotic and credible intervals are also established for each unknown quantity. Since the posterior density is complicated, the Markov chain using the Monte Carlo approach is utilized to get information from the whole marginal posterior densities and thus assess the acquired Bayesian point and interval estimations. Using four optimality criteria, the optimum censoring is given among competing progressive techniques. The effectiveness of the offered estimations is tested against numerous parameters using comprehensive Monte Carlo comparisons. Lastly, the practical utility of the GTL model is demonstrated through two applications using different real-world datasets collected from veterinary medicine and engineering reliability studies. Our findings state that the Bayes' setup outperforms classical approaches, particularly in small-sample settings, making the proposed methodology flexible and beneficial in concluding the study when the researcher's foremost concern is the total number of failed items.

OPEN ACCESS

Received: 29/03/2025

Accepted: 21/05/2025

Accepted: 22/09/2025

DOI
10.23967/j.rimni.2025.10.66081

Keywords:
Extended topp-leone
adaptive censoring
markovian samples
reliability
likelihood optimization
optimum plan
real-world applications

*Correspondence: Osama E. Abo-Kasem (osamaelsayederaki@gmail.com or o.e.abokasem@zu.edu.eg).

1 Introduction

The Topp-Leone (TL(ρ)) lifetime model, by Topp and Leone [1], seems easy to work with, but we don't know enough about how it's spread out compared to other types of probability models. Thus, the TL distribution can be used instead of the beta or Kumaraswamy distributions because its densities can be easily handled. Since the TL distribution provides a J-shaped frequency curve for $\rho < 1$, it is also known as the J-shaped distribution. Practical real-life situations such as engineering, biomedicine, economics, social sciences, etc., often involve studying things that have specific percentage data that are measured between 0 and 1. Sangsanit and Bodhisuwan [2] utilized the TL distribution as a generator in the T-X family of distributions (suggested by Alzaatreh et al. [3]) and introduced the TL generalized exponential distribution. Recently, using the power transformation considered by Gupta and Kundu [4], Shekhawat and Sharma [5] introduced a novel two-parameter generalized (extended) TL model, which is quite flexible and has numerous curves for both hazard and density functions. They also stated, using tissue damage fractions in blood at different concentrations, that the generalized-TL (GTL) provides an excellent fit compared to unit-Weibull, unit-gamma, Kumarswamy, and beta distributions. Henceforward, we shall refer to this model as GTL($\boldsymbol{\vartheta}$), where $\boldsymbol{\vartheta} = (\rho, \tau)^\top$. Suppose Y is a time random variable of a test item(s) follows GTL($\boldsymbol{\vartheta}$), then its probability density function (PDF) $f(\cdot)$, reliability function (RF) $R(\cdot)$, and hazard rate function (HRF) $h(\cdot)$, are given by

$$f(y; \boldsymbol{\vartheta}) = 2\rho\tau y^{\rho\tau-1}(1 - y^\tau)(2 - y^\tau)^{\rho-1}, \ 0 > y > 1, \ \rho, \tau > 0, \tag{1}$$

$$R(y; \boldsymbol{\vartheta}) = 1 - (y^\tau(2 - y^\tau))^\rho \tag{2}$$

and

$$h(y; \boldsymbol{\vartheta}) = \frac{2\rho\tau y^{\rho\tau-1}(1 - y^\tau)(2 - y^\tau)^{\rho-1}}{1 - (y^\tau(2 - y^\tau))^\rho}, \tag{3}$$

respectively. When $\tau \to 1$, the GTL model is reduced to the traditional TL model. Based on several options of ρ and τ, Fig. 1 displays the PDF (1) and HRF (3) of the GTL(ϑ) distribution. It shows that the density (1) function has a J–shaped when $\rho\tau < 1$, unimodal shape when $\rho\tau = 1$, or a decreasing shape when $\rho\tau > 1$. It also stands that the hazard (3) function has a bathtub (or increasing) shape.

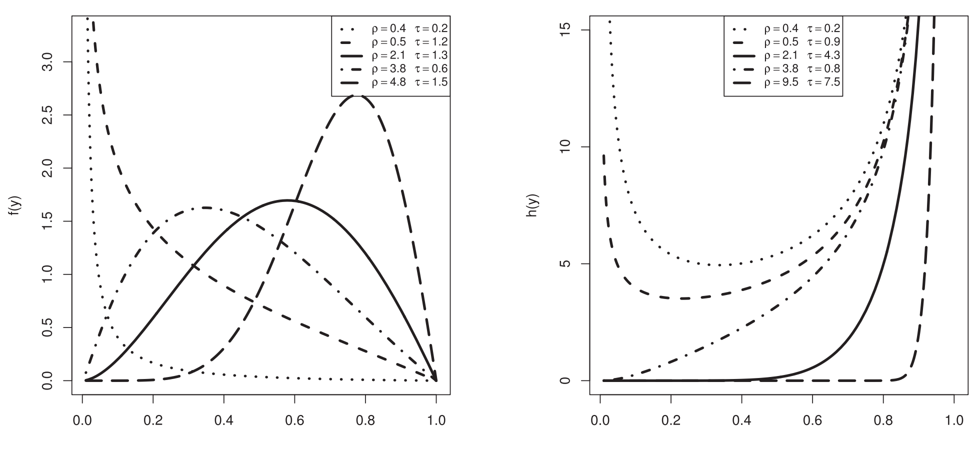

Figure 1: The GTL-PDF (left) and GTL-HRF (right) shapes

Adaptive progressively Type-II censoring (A-PT2C) is a method created by Ng et al. [6] to solve the main issue in progressive Type-II censoring (PT2C), which is that the accuracy of the statistical results is compromised due to the inadequate size of the censored sample. As a sequence, this scheme improves the efficiency of statistical analysis, ensures the experiment ends once a set number of failures occur, controls the total testing time, keeping it close to a predetermined time, and balances reliability in results with practical constraints on testing duration. It has been widely applied in many scientific sectors. This strategy starts with n (identical units being put to a test at $T = 0$), m (is a prefixed size of failed units), and $\mathbf{S} = (S_1, \ldots, S_m)$ (is a removal pattern). Following the recording of the first failure $Y_{1:m:n}$, the survived unit(s) S_1 (of $n-1$) are randomly removed from the test. The survived unit(s) S_2 (of $n-2-S_1$) are then eliminated at the second failure, $Y_{2:m:n}$, and so on. Towards the final stage, the test terminates at $Y_{m:m:m}$ with $\mathbf{S}$ if $Y_{m:m:m} < T$. Otherwise, pause the removal process for any surviving elements, i.e., $S_i = 0$ for $i = k+1, \ldots, m-1$, where k is the number of failures that occurred before T. Then, remove all surviving items S_m^* (where $S_m^* = n - m - \sum_{i=1}^{k} S_i$) and end the test at T.

Let $\mathbf{y} = \{y_{i:m:n}, S_i\}$ for $i = 1, 2, \ldots, m$, be an A-PT2C sample from a lifetime population, then the likelihood function (LF) can be represented as

$$\mathcal{L}(\boldsymbol{\vartheta}|\mathbf{y}) = D\prod_{i=1}^{m} f(y_{i:m:n};\boldsymbol{\vartheta})\prod_{i=1}^{k}[R(y_{i:m:n};\boldsymbol{\vartheta})]^{S_i}[R(y_{m:m:n};\boldsymbol{\vartheta})]^{S_m^*}, \tag{4}$$

where $D = \prod_{i=1}^{m}\left[n - i + 1 - \sum_{j=1}^{\max\{i-1,k\}} S_j\right]$.

This adjustment permits testing with diverse removals and guarantees the evaluation is completed with the appropriate size of failed items and within the specified time frame. From (4), several research have been developed in the literature; for example, see Liu and Gui [7], Kohansal and Bakouch [8], Elshahhat and Nassar [9], Du and Gui [10], Alotaibi et al. [11], Nassar et al. [12], Elshahhat and Nassar [13], Elshahhat et al. [14], Muhammed and Almetwally [15], El-Saeed and Abdellatif [16], and referenced cited therein.

Although there is a wide range of studies dealing with A-PT2C data, we have not encountered any effort that discusses the inferential analysis of the GTL distribution in the presence of the proposed strategy. Therefore, we can support this work by showing that (i) A-PT2C helps make parameter estimation better when there are not many observations, and (ii) GTL distribution can analyze various data types with varying failure rates. So, this work aims to:

- Derive the maximum likelihood estimators (MLEs) and asymptotic confidence intervals (ACIs) of the GTL parameters ρ, τ, $R(t)$, and $h(t)$ using the proposed censored sample.
- Drive the Bayes estimators and highest posterior density (HPD) intervals for all parameters using independent gamma priors and a squared-error loss (SEL) framework. All estimators developed by the Bayes setup cannot be solved analytically; therefore, Monte Carlo Markov Chain (MCMC) techniques are proposed.
- Identify the optimal PT2C design by applying different optimality measures.
- Evaluate the performance of the suggested approaches by root mean squared error, mean absolute bias, average interval length, and coverage probability through extensive Monte Carlo simulations.
- Analyze two genuine data sets to highlight the flexibility and practical applicability of the GTL model in distinct real applications.

The structure of the paper is as follows: Sections 2 and 3 present the derivation of likelihood and Bayes estimators, respectively. Section 4 outlines the Monte Carlo results, while Section 5 discusses optimal censoring. Section 6 explores two genuine applications, and the conclusion is provided in Section 7.

2 Likelihood Estimators

The likelihood method in estimation provides a consistent and efficient way to estimate model parameters by maximizing the probability of observing the given data. It also allows for flexible modeling and inference under both simple and complex statistical models. From (1) and (2), the LF for the observed A-PT2C $\mathbf{y}$ data, where $y_i = y_{i:m:n}$, becomes

$$\mathcal{L}(\boldsymbol{\vartheta}|\mathbf{y}) \propto\propto (\rho\tau)^m \prod_{i=1}^{m} y_i^{\rho\tau} \left(1-y_i^{\tau}\right)\left(2-y_i^{\tau}\right)^{\rho-1} \prod_{i=1}^{k} \left(1-\xi_i^{\rho}\right)^{S_i} \left(1-\xi_m^{\rho}\right)^{S_m^*}, \tag{5}$$

where $\xi_i = y_i^{\tau}\left(2-y_i^{\tau}\right)$ for $i = 1, 2, \ldots, k$.

Subsequently, from (5), we get the log-LF (denoted by $\mathcal{L}^{\bullet}(\cdot) \propto \mathcal{L}(\cdot)$) as

$$\mathcal{L}^{\bullet}(\boldsymbol{\vartheta}|\mathbf{y}) \propto m\log(\rho\tau) + \rho\tau\sum_{i=1}^{m}\log(y_i) + \sum_{i=1}^{m}\left[\log\left(1-y_i^{\tau}\right) + (\rho-1)\log\left(2-y_i^{\tau}\right)\right]$$
$$+\sum_{i=1}^{k} S_i \log\left(1-\xi_i^{\rho}\right) + S_m^* \log\left(1-\xi_m^{\rho}\right). \tag{6}$$

By simultaneously solving the next two normal (nonlinear) formulae, the MLEs $\check{\rho}$ and $\check{\tau}$ of ρ and τ, respectively, may be provided:

$$\frac{\partial\mathcal{L}^{\bullet}}{\partial\rho} = m\rho^{-1} + \sum_{i=1}^{m}\left[\tau\log(y_i) + \log\left(2-y_i^{\tau}\right)\right]$$
$$-\sum_{i=1}^{k} S_i\xi_i^{\rho}\log(\xi_i)\left(1-\xi_i^{\rho}\right)^{-1} - S_m^*\xi_m^{\rho}\log(\xi_m)\left(1-\xi_m^{\rho}\right)^{-1} \tag{7}$$

and

$$\frac{\partial\mathcal{L}^{\bullet}}{\partial\tau} = m\tau^{-1} + \rho\sum_{i=1}^{m}\log(y_i) - \sum_{i=1}^{m} y_i^{\tau}\log(y_i)\left[\left(1-y_i^{\tau}\right)^{-1} + (\rho-1)\left(2-y_i^{\tau}\right)^{-1}\right]$$
$$-\rho\left[\sum_{i=1}^{k} S_i\xi_i^{\rho-1}\xi_i^{\circ}\left(1-\xi_i^{\rho}\right)^{-1} + S_m^*\xi_m^{\rho-1}\xi_m^{\circ}\left(1-\xi_m^{\rho}\right)^{-1}\right], \tag{8}$$

where $\xi_i^{\circ} = 2y_i^{\tau}\log(y_i)\left(1-y_i^{\tau}\right)$ for $i = 1, 2, \ldots, k$.

It is noted that the MLEs $\check{\rho}$ and $\check{\tau}$ in (7) and (8), respectively, cannot be formulated in explicit solutions. After specifying the values of T, m, and $\mathbf{S}$, the MLEs $\check{\rho}$ and $\check{\tau}$ can be acquired via the Newton-Raphson iteration method. To handle this problem, the 'maxLik' package (by Henningsen and Toomet [17]) is supplied.

Upon obtaining the estimates of ρ and τ, by performing the invariance property of $\check{\rho}$ and $\check{\tau}$, the MLEs $\check{R}(t)$ and $\check{h}(t)$ of $R(t)$ and $h(t)$ at a certain time $t > 0$ are produced as

$$\check{R}(t) = 1 - \left(t^{\check{\tau}}(2 - t^{\check{\tau}})\right)^{\check{\rho}} \text{ and } \check{h}(t) = \frac{2\check{\rho}\check{\tau}t^{\check{\rho}\check{\tau}-1}(1 - t^{\check{\tau}})(2 - t^{\check{\tau}})^{\check{\rho}-1}}{1 - (t^{\check{\tau}}(2 - t^{\check{\tau}}))^{\check{\rho}}},$$

respectively.

Remark 1: From (5) we have expanded some related works in literature, such as:

- Bayoud [18] results in the case of PT2C from TL model (for ρ only) when $T \to \infty$ and $\tau \to 1$;
- Feroze et al. [19] using PT2C from TL model when $T \to \infty$ and $\tau \to 1$;
- Ilhan [20] using PT2C from TL model when $T \to \infty$ and $\rho \to 1$;
- Feroze and Aslam [21] as well as Arora et al. [22] using Type-II censoring from TL model when $S_i = 0$ for $i = 1, 2, \ldots, m-1$, $T \to \infty$, and $\tau \to 1$.

Now, to construct the $(1-\gamma)100\%$ ACI of ρ, τ, $R(t)$ or $h(t)$, we need to find their asymptotic properties. The Fisher information (FI) of $\check{\boldsymbol{\vartheta}}$ cannot be used directly to build the variance-covariance (VC) matrix. This is due to the nonlinear form in (5). So, by replacing $\boldsymbol{\vartheta}$ with its $\check{\boldsymbol{\vartheta}}$, we can estimate VC matrix ($\mathbf{I}_{2\times2}^{-1}(\boldsymbol{\vartheta})$) by $\mathbf{I}_{2\times2}^{-1}(\check{\boldsymbol{\vartheta}})$ as

$$\mathbf{I}_{2\times2}^{-1}(\check{\boldsymbol{\vartheta}}) = \begin{bmatrix} -\mathcal{I}_{11} & -\mathcal{I}_{12} \\ -\mathcal{I}_{21} & -\mathcal{I}_{22} \end{bmatrix}^{-1}_{(\rho,\tau)=(\check{\rho},\check{\tau})} = \begin{bmatrix} \check{\sigma}_{11} & \check{\sigma}_{12} \\ \check{\sigma}_{21} & \check{\sigma}_{22} \end{bmatrix}, \tag{9}$$

where

$$\mathcal{I}_{11} = -m\rho^{-2} - \sum_{i=1}^{k} S_i \xi_i^{\rho} \log^2(\xi_i) \left\{ \xi_i^{\rho} (\bar{\xi}_i^{\rho})^{-2} + (\bar{\xi}_i^{\rho})^{-1} \right\} - S_m^* \xi_m^{\rho} \log^2(\xi_m) \left\{ \xi_m^{\rho} (\bar{\xi}_m^{\rho})^{-2} + (\bar{\xi}_m^{\rho})^{-1} \right\},$$

$$\begin{aligned}
\mathcal{I}_{22} = {} & -m\tau^{-2} - \sum_{i=1}^{m} y_i^{2\tau} \log^2(y_i) \left[\left(1 - y_i^{\tau}\right)^{-2} + (\rho - 1)\left(2 - y_i^{\tau}\right)^{-2} \right] \\
& - \sum_{i=1}^{m} y_i^{\tau} \log^2(y_i) \left[\left(1 - y_i^{\tau}\right)^{-1} + (\rho - 1)\left(2 - y_i^{\tau}\right)^{-1} \right] \\
& - \rho \sum_{i=1}^{k} S_i \xi_i^{\rho-1} \left(\xi_i^{\circ}\right)^2 (\bar{\xi}_i^{\rho})^{-1} \left\{ \rho \xi_i^{\rho-1} + (\rho - 1)\xi_i^{-1} + \xi_i^{\circ\circ} \right\} \\
& - \rho S_m \xi_m^{\rho-1} \left(\xi_m^{\circ}\right)^2 (\bar{\xi}_m^{\rho})^{-1} \left\{ \rho \xi_m^{\rho-1} + (\rho - 1)\xi_m^{-1} + \xi_m^{\circ\circ} \right\},
\end{aligned}$$

and

$$\begin{aligned}
\mathcal{I}_{12} = {} & \sum_{i=1}^{m} \log(y_i) - \sum_{i=1}^{m} y_i^{\tau} \log(y_i) \left(2 - y_i^{\tau}\right)^{-1} - \sum_{i=1}^{k} S_i \xi_i^{\rho-1} \xi_i^{\circ} (\bar{\xi}_i^{\rho})^{-1} \left[1 + \rho \log(\xi_i) \left\{ 1 + \xi_i^{\rho} (\bar{\xi}_i^{\rho})^{-1} \right\} \right] \\
& - S_m \xi_m^{\rho-1} \xi_m^{\circ} (\bar{\xi}_m^{\rho})^{-1} \left[1 + \log(\xi_m) \left\{ 1 + \xi_m^{\rho} (\bar{\xi}_m^{\rho})^{-1} \right\} \right],
\end{aligned}$$

where $\bar{\xi}_i^{\rho} = (1 - \xi_i^{\rho})$ and $\xi_i^{\circ\circ} = 2y_i^{\tau} \log^2(y_i)\left(1 - y_i^{\tau}\right)^2$, $i = 1, 2, \ldots, k$.

We now create the two $100(1-\gamma)\%$ ACI bounds of ρ and τ as follows:

$$\check{\rho} \mp z_{\frac{\gamma}{2}} \sqrt{\check{\sigma}_{11}} \quad \text{and} \quad \check{\tau} \mp z_{\frac{\gamma}{2}} \sqrt{\check{\sigma}_{22}},$$

respectively, where $\breve{\sigma}_{ii}$ for $i = 1, 2$ are provided in (9) and $z_{\frac{\gamma}{2}}$ is $\left(\frac{\gamma}{2}\right)$th upper-percentile point of the standard normal distribution.

Further, to create the $100(1-\gamma)\%$ ACIs of $R(t)$ or $h(t)$, the variance of $\breve{R}(t)$ and $\breve{h}(t)$ must be derived first. As stated by Wasserman [23], the associated variances of $R(t)$ and $h(t)$ (say, $\breve{\sigma}_R$ and $\breve{\sigma}_h$, respectively) can be approximated at $\boldsymbol{\vartheta} = \breve{\boldsymbol{\vartheta}}$ as

$$\breve{\sigma}_R = \mathcal{A}_1 \mathbf{I}_{2\times 2}^{-1}(\breve{\boldsymbol{\vartheta}}) \mathcal{A}_1^\top \quad \text{and} \quad \breve{\sigma}_h = \mathcal{A}_2 \mathbf{I}_{2\times 2}^{-1}(\breve{\boldsymbol{\vartheta}}) \mathcal{A}_2^\top, \tag{10}$$

respectively, where $\mathcal{A}_i,\ i = 1, 2$, denote the first derivatives of $R(t)$ and $h(t)$, respectively, with respect to ρ and τ.

Now, from (10), the $100(1-\gamma)\%$ ACI bounds of $R(t)$ and $h(t)$ are

$$\breve{R}(t) \mp z_{\frac{\gamma}{2}} \sqrt{\breve{\sigma}_R} \quad \text{and} \quad \breve{h}(t) \mp z_{\frac{\gamma}{2}} \sqrt{\breve{\sigma}_h},$$

respectively.

3 Bayes Estimators

In the Bayesian framework, we can integrate our prior understanding of a parameter we seek to gain more insight into. The choice of prior knowledge for unknown parameter(s) is a significant challenge in Bayesian inference. In this part, the gamma prior is beneficial in Bayesian frameworks because it simplifies calculations through conjugacy with common likelihoods. It also provides various shapes based on parameter values, is flexible, and allows the flexibility to model a wide range of prior beliefs. In this regard, to obtain the Bayes and $100(1-\gamma)\%$ HPD interval estimators, assuming that ρ and τ are independent and random variables, we use gamma priors to offer more information, such as $\rho \sim \rho^{\alpha_1-1}e^{-\alpha_1\rho},\ \rho > 0$ and $\tau \sim \tau^{\alpha_2-1}e^{-\lambda_2\tau},\ \tau > 0$. The prior PDF of ρ and τ, say $\Pi_L(\cdot)$, is

$$\Pi_L(\boldsymbol{\vartheta}) \propto \rho^{\alpha_1-1}\tau^{\alpha_2-1}e^{-(\lambda_1\rho+\lambda_2\tau)}, \tag{11}$$

where $\alpha_i, \lambda_i > 0,\ i = 1, 2$, refer the hyper-parameters.

From (5) and (11), the posterior PDF of ρ and τ, denoted by $\Pi_L^\bullet$, becomes

$$\Pi_L^\bullet(\boldsymbol{\vartheta}|\mathbf{y}) \propto \rho^{m+\alpha_1-1}\tau^{m+\alpha_2-1}e^{-\left(\rho\lambda_1^*+\tau\lambda_2^*\right)} \prod_{i=1}^{k} \left(1-\xi_i^\rho\right)^{S_i} \left(1-\xi_m^\rho\right)^{S_m^*}, \tag{12}$$

where

$$\lambda_1^* = \lambda_1 + \tau \sum_{i=1}^{m} \log(y_i) - \sum_{i=1}^{m} \log\left(2-y_i^\tau\right) \text{ and } \lambda_2^* = \lambda_2 - \sum_{i=1}^{m} \log\left(1-y_i^\tau\right) + \sum_{i=1}^{m} \log\left(2-y_i^\tau\right).$$

Remark 2: The closed (analytical) expressions of ρ and τ, from (12), cannot be obtained. Consequently, following Gelman et al. [24], we propose performing the Metropolis-Hastening (MH) technique to compute the Bayes (or HPD interval) estimators of ρ, τ, $R(t)$, and $h(t)$.

To do this, the posterior PDFs of ρ and τ (denoted by $\Pi_L^1(\cdot)$ and $\Pi_L^2(\cdot)$) must be first derived as

$$\Pi_L^1(\rho|\tau, \mathbf{y}) \propto \rho^{m+\alpha_1-1}e^{-\rho\lambda_1^*} \prod_{i=1}^{k} \left(1-\xi_i^\rho\right)^{S_i} \left(1-\xi_m^\rho\right)^{S_m^*} \tag{13}$$

and

$$\Pi_L^2(\tau|\rho,\mathbf{y}) \propto \tau^{m+\alpha_2-1}e^{-\left(\rho\lambda_1^*+\tau\lambda_2^*\right)}\prod_{i=1}^{k}\left(1-\xi_i^{\rho}\right)^{S_i}\left(1-\xi_m^{\rho}\right)^{S_m^*}, \tag{14}$$

respectively.

The entire distributions of ρ and τ are unable to be statistically adapted to any usual distribution, as we anticipated. Fig. 2, which uses data visualization, shows that the ideal density of ρ or τ corresponds to the normal density. In Bayesian estimation, determining whether the conditional posteriors are log-concave is important, as many MCMC sampling algorithms rely on this property. Using the same data as in Fig. 2, Fig. 3 shows that the conditional posterior densities for ρ and τ exhibit clear log-concavity, as evidenced by the unimodal and downward-curving shapes of their respective log-posterior plots. We now propose the following MH steps:

Step 1. Put $\zeta = 1$.

Step 2. Set $\left(\rho^{(0)},\tau^{(0)}\right) = (\check{\rho},\check{\tau})$.

Step 3. Generate $\rho^\star$ and $\tau^\star$ from (13) and (14) using normal distributions $N\left(\check{\rho},\check{\sigma}_{11}\right)$ and $N\left(\check{\tau},\check{\sigma}_{22}\right)$, respectively, then follow steps (a)–(e):

(a) Obtain $G_1 = \dfrac{\Pi_L^1(\rho^\star|\tau^{(\zeta-1)},\mathbf{y})}{\Pi_L^1(\rho^{(\zeta-1)}|\tau^{(\zeta-1)},\mathbf{y})}$ and $G_2 = \dfrac{\Pi_L^2(\tau^\star|\rho^{(\zeta)},\mathbf{y})}{\Pi_L^2(\tau^{(\zeta-1)}|\rho^{(\zeta)},\mathbf{y})}$.

(b) Obtain $g_i = \min\{1, G_i\}$ for $\zeta = 1, 2$.

(c) Obtain u_i for $\zeta = 1, 2$, from uniform $U(0, 1)$ distribution.

(d) If $u_1 \leqslant g_1$, set $\rho^{(\zeta)} = \rho^*$ else set $\rho^{(\zeta)} = \rho^{(\zeta-1)}$.

(e) If $u_2 \leqslant g_2$, set $\tau^{(\zeta)} = \tau^*$ else set $\tau^{(\zeta)} = \tau^{(\zeta-1)}$.

Step 4. Obtain $R^{(\zeta)}(t)$ and $h^{(\zeta)}(t)$ as

$$R^{(\zeta)}(t) = 1-\left(t^{\tau^{(\zeta)}}(2-t^{\tau^{(\zeta)}})\right)^{\rho^{(\zeta)}}$$

and

$$h^{(\zeta)}(t) = \frac{2\rho^{(\zeta)}\tau^{(\zeta)}t^{\rho^{(\zeta)}\tau^{(\zeta)}-1}(1-t^{\tau^{(\zeta)}})(2-t^{\tau^{(\zeta)}})^{\rho^{(\zeta)}-1}}{1-\left(t^{\tau^{(\zeta)}}(2-t^{\tau^{(\zeta)}})\right)^{\rho^{(\zeta)}}}.$$

Step 5. Set $\zeta = \zeta + 1$.

Step 6. Redo Steps 3–5 $\mathcal{V}$ times to get

$$\left[\rho^{(1)},\tau^{(1)},R^{(1)}(t),h^{(1)}(t)\right],\ldots,\left[\rho^{(\mathcal{V})},\tau^{(\mathcal{V})},R^{(\mathcal{V})}(t),h^{(\mathcal{V})}(t)\right].$$

Step 7. Calculate the Bayes estimates of ρ as

$$\bar{\rho}_L = \frac{1}{\bar{\mathcal{V}}}\sum_{\zeta=\mathcal{V}^\circ+1}^{\mathcal{V}}\rho^{(\zeta)},$$

where $\bar{\mathcal{V}} = \mathcal{V}-\mathcal{V}^\circ$ is burn-in.

Step 8. Create the $100(1-\gamma)\%$ HPD interval of ρ as

(a) Order the MCMC draws of $\rho^{(\zeta)}$ for $\zeta = \mathcal{V}^{\circ}+1, \mathcal{V}^{\circ}+2, \ldots, \mathcal{V}^{\circ}$ as

$$\rho_{(\mathcal{V}^{\circ}+1)}, \rho_{(\mathcal{V}^{\circ}+2)}, \ldots, \rho_{(\mathcal{V})}.$$

(b) Calculate the $100(1-\gamma)\%$ HPD interval of ρ, according to Chen and Shao [25], as

$(\rho_{(\zeta^*)}, \rho_{(\zeta^*+(1-\gamma)\bar{\mathcal{V}})})$,

where $\zeta^* = \mathcal{V}^{\circ}+1, \mathcal{V}^{\circ}+2, \ldots, \mathcal{V}$ is chosen such that

$\rho_{(\zeta^*+[(1-\gamma)(\mathcal{V}-\mathcal{V}^{\circ})])} - \rho_{(\zeta^*)} = \min_{1\leqslant\zeta\leqslant\gamma\bar{\mathcal{V}}} (\rho_{(\zeta+[(1-\gamma)\bar{\mathcal{V}}])} - \rho_{(\zeta)})$.

Step 9. Redo Steps 7–8 for τ, $R(t)$, and $h(t)$.

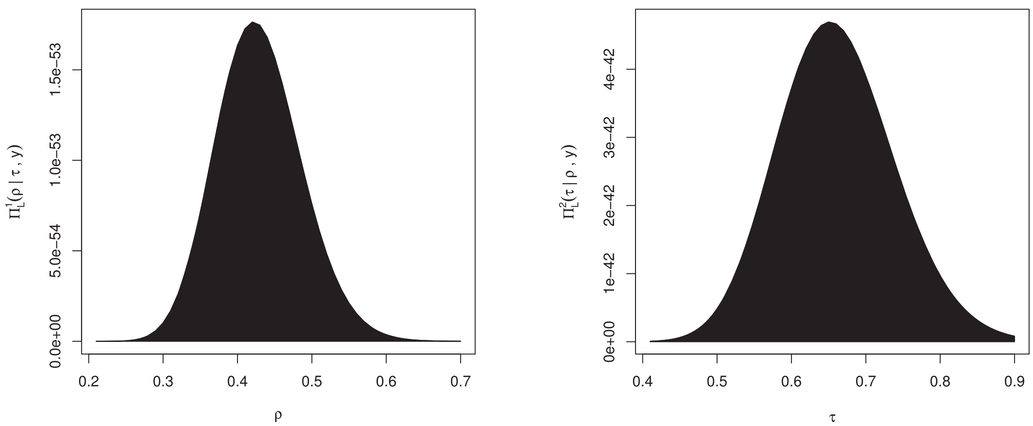

Figure 2: Conditional density plots of ρ (left) and τ (right)

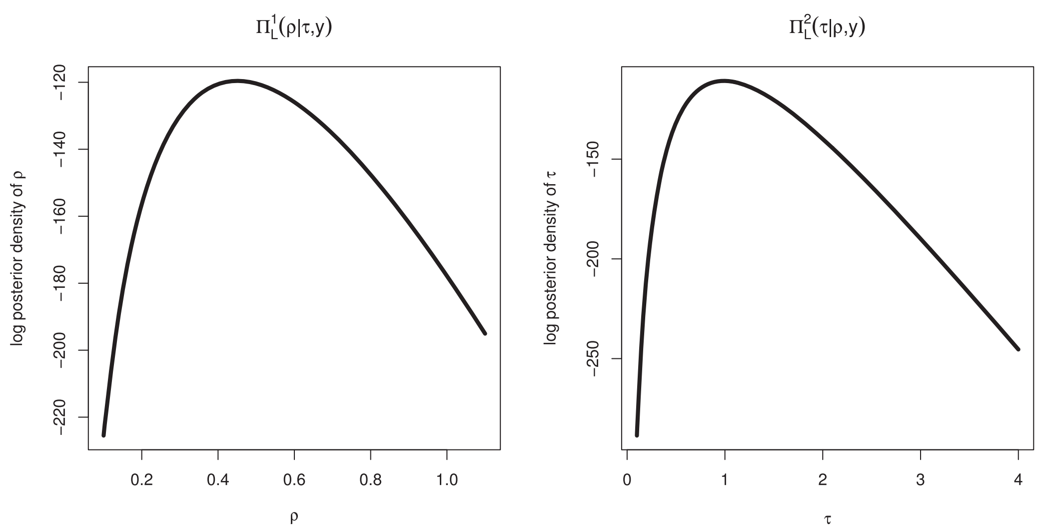

Figure 3: Conditional density plots of ρ (left) and τ (right)

4 Numerical Comparisons

In this section, using a variety of Monte Carlo simulations, the accuracy of the suggested estimators and the time indices created in the previous parts are evaluated.

4.1 Simulation Designs

Making use of different choices of T, n, m, and $\mathbf{S}$, large 1000 A-PT2C samples are collected from GTL(0.5, 1.5). At $t = 0.1$, the genuine values of $R(t)$ and $h(t)$ are used as 0.7505 and 2.4531, respectively. For each group of T(=0.4,0.8) and n(=50,80), we assign the value of m as a failure percent (FP) such as $\frac{m}{n} \times 100\%$ (=40%, 80%). Several deigns of $\mathbf{S}$ are also utilized, namely:

Censoring[1] : $(n - m, 0^{m-1})$;

Censoring[2] : $(0^{(\frac{m}{2}-1)}, n - m, 0^{\frac{m}{2}})$;

and

Censoring[3] : $(0^{m-1}, n - m)$,

where $(1, 1, 1, 2, 2, 2)$ is denoted by $(1^3, 2^3)$ for simplicity. It is better to note that the suggested designs (Censoring[i] for $i = 1, 2, 3$) represent the left, middle, and right censoring plans, respectively.

Briefly, to get an A-PT2C dataset from the GTL($\boldsymbol{\vartheta}$) distribution, do:

Step 1: Set the assigned values of GTL(ρ, τ).

Step 2: Simulate a PT2C sample (say (Y_i, S_i)), for $i = 1, 2, \ldots, m$, as:

(i) Simulate μ independent items (say $\mu_1, \mu_2, \ldots, \mu_m$) from uniform $U(0, 1)$ distribution.

(ii) Set $\epsilon_i = \mu_i^{\left(i+\sum_{j=m-i+1}^{m} S_j\right)^{-1}}$, for $i = 1, 2, \ldots, m$.

(iii) Set $U_i = 1 - \epsilon_m \epsilon_{m-1} \cdots \epsilon_{m-i+1}$ for $i = 1, 2, \ldots, m$.

(iv) Set $Y_i = \left(1 - \sqrt{1 - u_i^{\rho^{-1}}}\right)^{\tau^{-1}}$, $i = 1, 2, \ldots, m$, the PT2C from GTL(ρ, τ) is collected.

Step 3: Find k and ignore Y_i for $i = k + 2, \ldots, m$.

Step 4: Use a truncated distribution $f(y)[R(y_{k+1})]^{-1}$ to get $Y_{k+2}, \ldots, Y_m$.

Once the necessary 1000 A-PT2C samples are gathered, the frequentist and Bayes' estimates (along with their 95% ACI and HPD interval estimates) of ρ, τ, $R(t)$, and $h(t)$ are obtained by R 4.2.2 software. To see the influence of the gamma priors, setting $\mathcal{V} = 12{,}000$ and $\mathcal{V}^{\circ} = 2000$, two informative sets of the hyper-parameters $(\alpha_1, \alpha_2, \lambda_1, \lambda_2)$ are used; namely, P1: $(2.5, 7.5, 5, 5)$ and P2: $(5, 15, 10, 10)$. Following Kundu [26], the suggested values of (α_i, λ_i) for $i = 1, 2$, are set to be the prior expectation that corresponds to the actual value of GTL(ρ, τ). All Bayes calculations are done with the 'coda' package introduced by Plummer et al. [27].

Computationally, the average point estimates (Av.PEs) of ρ (for instance) is provided by

$$\text{Av.PE}(\acute{\rho}) = \frac{1}{1000} \sum_{\varsigma=1}^{1000} \acute{\rho}^{[\varsigma]},$$

where $\acute{\rho}^{[\varsigma]}$ is an estimate of ρ computed from jth sample.

Two metrics are used to examine the accuracy of point estimates of ρ, namely:

(i) Root Mean Squared-Error (RMSE):

$$\mathrm{RMSE}(\acute{\rho}) = \sqrt{\frac{1}{1000}\sum_{i=\varsigma}^{1000}\left(\acute{\rho}^{(j)} - \rho\right)^2},$$

(ii) Mean Absolute Bias (MAB):

$$\mathrm{MAB}(\acute{\rho}) = \frac{1}{1000}\sum_{i=\varsigma}^{1000}\left|\acute{\rho}^{[\varsigma]} - \rho\right|.$$

Additionally, two metrics are used to examine the accuracy of 95% interval estimates of ρ, namely:

(i) Average Interval Length (AIL):

$$\mathrm{AIL}_{95\%}(\rho) = \frac{1}{1000}\sum_{i=\varsigma}^{1000}\left(\mathcal{U}_{\acute{\rho}[\varsigma]} - \mathcal{L}_{\acute{\rho}[\varsigma]}\right)$$

(ii) Coverage Percentage (CP):

$$\mathrm{CP}_{95\%}(\rho) = \frac{1}{1000}\sum_{i=\varsigma}^{1000}\aleph_{\left(\mathcal{L}_{\acute{\rho}[\varsigma]};\mathcal{U}_{\acute{\rho}[\varsigma]}\right)}(\rho),$$

respectively, where $\aleph(\cdot)$ is the indicator operator, and $(\mathcal{L}(\cdot),\mathcal{U}(\cdot))$ denote the (lower, upper) interval bounds. In Tables 1–4, the Av.PEs, RMSEs, and MABs are listed in the first, second, and third columns, respectively. The AILs and CPs (presented in Tables 5–8) are listed in the first and second columns, respectively.

Table 1: The point evaluations of ρ

n[FP%]	Scheme	MLE			MCMC[P1]			MCMC[P2]		
					$T = 0.4$					
50[40%]	1	0.8933	1.8079	1.7892	0.4841	0.5460	0.6393	0.5799	0.2182	0.2550
	2	0.7343	1.6575	1.5796	0.4381	0.5240	0.5910	0.5751	0.2053	0.2398
	3	0.7867	1.5057	1.4125	0.4139	0.5015	0.5488	0.5850	0.1962	0.2252
50[80%]	1	0.6925	1.4081	1.2870	0.5171	0.4936	0.4795	0.4968	0.1842	0.1938
	2	0.6458	1.2984	1.2163	0.4861	0.4925	0.4479	0.4980	0.1748	0.1634
	3	0.6858	1.1808	1.1714	0.4757	0.4645	0.4312	0.4974	0.1504	0.1433
80[40%]	1	0.5941	1.0577	1.1243	0.5148	0.4034	0.3922	0.4914	0.1319	0.1276
	2	0.6246	0.9132	0.8994	0.5029	0.3744	0.3502	0.4932	0.1148	0.1123
	3	0.6054	0.8592	0.7616	0.5235	0.3424	0.3293	0.5050	0.1083	0.0821
80[80%]	1	0.5123	0.7486	0.6523	0.5120	0.3132	0.3028	0.5353	0.0861	0.0713
	2	0.5925	0.6549	0.5490	0.5026	0.2712	0.2862	0.5403	0.0784	0.0609
	3	0.4992	0.5411	0.4105	0.4860	0.2518	0.2449	0.5422	0.0567	0.0542

(Continued)

Table 1 (continued)

n[FP%]	Scheme	MLE			MCMC[P1]			MCMC[P2]		
					$T = 0.8$					
50[40%]	1	0.8140	1.2500	1.6627	0.4463	0.5089	0.5512	0.5798	0.1822	0.2170
	2	0.8135	1.1339	1.4635	0.3942	0.4941	0.5220	0.5745	0.1723	0.1955
	3	0.7187	1.0024	1.3658	0.4139	0.4799	0.4765	0.5850	0.1605	0.1690
50[80%]	1	0.6993	0.9264	1.1542	0.4705	0.4756	0.4549	0.4958	0.1484	0.1426
	2	0.5920	0.8841	0.9884	0.5263	0.4686	0.4231	0.4953	0.1362	0.1247
	3	0.4865	0.8658	0.8471	0.5169	0.4451	0.3861	0.5144	0.1244	0.1090
80[40%]	1	0.5165	0.8105	0.7563	0.4856	0.3976	0.3480	0.4892	0.1028	0.0972
	2	0.4713	0.7963	0.6707	0.5073	0.3238	0.3246	0.4922	0.0879	0.0832
	3	0.6507	0.7774	0.5447	0.4860	0.3132	0.2877	0.5158	0.0659	0.0732
80[80%]	1	0.6846	0.6214	0.4272	0.4926	0.2822	0.2662	0.5387	0.0586	0.0659
	2	0.4881	0.5436	0.3783	0.4741	0.2542	0.2314	0.5411	0.0515	0.0504
	3	0.5397	0.4860	0.3391	0.5062	0.2396	0.1901	0.5516	0.0476	0.0444

Table 2: The point evaluations of τ

n[FP%]	Scheme	MLE			MCMC[P1]			MCMC[P2]		
					$T = 0.4$					
50[40%]	1	1.8838	1.8323	2.1147	2.1539	1.1723	1.1817	1.5763	0.8419	0.7169
	2	1.9625	2.0036	2.3733	2.1847	1.2458	1.3190	1.5693	0.8743	0.7423
	3	2.1977	2.1634	2.6142	2.2373	1.5520	1.4802	1.5695	0.9062	0.7771
50[80%]	1	1.9942	1.4280	1.8723	2.6902	0.9469	0.9105	1.5697	0.6987	0.6581
	2	2.0386	1.5312	1.9861	2.5192	1.0080	0.9953	1.5604	0.7405	0.6974
	3	1.9737	1.7526	2.0680	2.5218	1.0722	1.0192	1.5628	0.8187	0.7015
80[40%]	1	1.8270	1.0945	1.5942	2.9802	0.8124	0.7550	1.5777	0.6221	0.5725
	2	2.0361	1.1236	1.6990	2.3694	0.8965	0.7956	1.5573	0.6451	0.6042
	3	1.8350	1.2441	1.7770	2.4952	0.9146	0.8698	1.5626	0.6706	0.6260
80[80%]	1	2.0194	0.8304	0.8590	2.2540	0.5340	0.4827	1.5156	0.4021	0.3338
	2	2.1442	0.8875	1.0364	1.9684	0.6606	0.6714	1.5096	0.4722	0.3644
	3	1.9071	0.9261	1.3868	1.8198	0.7912	0.7029	1.5039	0.5470	0.4380
					$T = 0.8$					
50[40%]	1	2.2872	1.6552	1.9233	2.1539	1.0821	0.9728	1.5763	0.6660	0.5658
	2	2.7626	1.7150	2.0326	2.0876	1.1005	1.0556	1.5685	0.6971	0.5705
	3	2.8781	1.8693	2.1666	2.1549	1.1687	1.1154	1.5691	0.7250	0.6178
50[80%]	1	1.5392	1.0025	1.6810	2.6154	0.9184	0.8719	1.5670	0.5610	0.4729
	2	1.8213	1.1814	1.8387	2.4727	0.9872	0.9353	1.5585	0.5872	0.5057

(Continued)

Table 2 (continued)

n[FP%]	Scheme	MLE			MCMC[P1]			MCMC[P2]		
	3	2.1977	1.4918	1.8790	2.3715	1.0132	0.9650	1.5586	0.6035	0.5382
80[40%]	1	1.9744	0.8095	1.3483	2.5556	0.7083	0.6126	1.5673	0.4757	0.3860
	2	1.8482	0.8595	1.4244	2.4647	0.7682	0.6714	1.5583	0.5176	0.4168
	3	1.6570	0.9632	1.4924	2.4350	0.7912	0.7250	1.5591	0.5377	0.4689
80[80%]	1	1.8303	0.5744	0.7880	1.9929	0.4807	0.3660	1.5194	0.3168	0.2644
	2	1.9486	0.7019	0.8659	1.8429	0.6160	0.4241	1.5041	0.3437	0.2969
	3	2.0145	0.7433	1.0528	1.9024	0.6706	0.5382	1.5042	0.3877	0.3250

Table 3: The point evaluations of $R(t)$

n[FP%]	Scheme	MLE			MCMC[P1]			MCMC[P2]		
					$T = 0.4$					
50[40%]	1	0.7496	0.1718	0.1330	0.7911	0.1394	0.1194	0.8162	0.1199	0.1093
	2	0.7508	0.1541	0.1196	0.7824	0.1269	0.1119	0.8136	0.1096	0.1046
	3	0.7936	0.1371	0.1142	0.8042	0.1164	0.1050	0.8204	0.1068	0.0925
50[80%]	1	0.7543	0.1165	0.1054	0.7172	0.1059	0.1005	0.7646	0.0961	0.0864
	2	0.7550	0.1096	0.0981	0.7224	0.0877	0.0908	0.7648	0.0785	0.0762
	3	0.8708	0.1027	0.0873	0.7255	0.0768	0.0804	0.7668	0.0641	0.0699
80[40%]	1	0.7513	0.0904	0.0760	0.7195	0.0657	0.0713	0.7607	0.0531	0.0656
	2	0.7532	0.0855	0.0677	0.7323	0.0584	0.0564	0.7606	0.0468	0.0631
	3	0.8377	0.0803	0.0635	0.7474	0.0445	0.0456	0.7741	0.0403	0.0360
80[80%]	1	0.7549	0.0760	0.0532	0.7648	0.0407	0.0416	0.7729	0.0359	0.0345
	2	0.7548	0.0543	0.0481	0.7714	0.0385	0.0371	0.7775	0.0270	0.0334
	3	0.8307	0.0487	0.0430	0.7746	0.0327	0.0336	0.7801	0.0281	0.0255
					$T = 0.8$					
50[40%]	1	0.7445	0.1358	0.1248	0.7888	0.1169	0.1094	0.8160	0.0750	0.0991
	2	0.7479	0.1222	0.1154	0.7787	0.1068	0.1003	0.8131	0.0708	0.0915
	3	0.7935	0.1158	0.1092	0.8042	0.0971	0.0883	0.8204	0.0676	0.0806
50[80%]	1	0.7518	0.1090	0.0946	0.7115	0.0885	0.0780	0.7627	0.0499	0.0677
	2	0.7535	0.0980	0.0851	0.7186	0.0819	0.0715	0.7624	0.0467	0.0603
	3	0.7831	0.0861	0.0805	0.7472	0.0717	0.0675	0.7775	0.0422	0.0560
80[40%]	1	0.7497	0.0820	0.0693	0.7159	0.0609	0.0618	0.7582	0.0376	0.0485
	2	0.7509	0.0777	0.0581	0.7321	0.0517	0.0483	0.7602	0.0340	0.0403
	3	0.7822	0.0720	0.0518	0.7624	0.0404	0.0415	0.7786	0.0333	0.0315

(Continued)

Table 3 (continued)

n[FP%]	Scheme	MLE			MCMC[P1]			MCMC[P2]		
80[80%]	1	0.7527	0.0695	0.0438	0.7683	0.0387	0.0367	0.7751	0.0279	0.0283
	2	0.7530	0.0447	0.0413	0.7701	0.0369	0.0332	0.7765	0.0247	0.0238
	3	0.7710	0.0386	0.0374	0.7837	0.0341	0.0307	0.7869	0.0242	0.0211

Table 4: The point evaluations of $h(t)$

n[FP%]	Scheme	MLE			MCMC[P1]			MCMC[P2]		
					$T = 0.4$					
50[40%]	1	2.0813	0.7125	0.5420	1.9913	0.4796	0.3796	1.9759	0.4657	0.3652
	2	2.5686	0.7459	0.5815	2.1211	0.5295	0.4455	2.0255	0.4864	0.4277
	3	2.5375	0.7774	0.6247	2.0546	0.5684	0.4975	2.0073	0.5164	0.4458
50[80%]	1	1.8404	0.6256	0.4594	2.3829	0.3652	0.2763	2.3327	0.3785	0.2426
	2	2.4524	0.6499	0.5067	2.4187	0.3921	0.2916	2.3479	0.4125	0.2798
	3	2.4564	0.6791	0.5233	2.4437	0.4303	0.3199	2.3483	0.4426	0.3125
80[40%]	1	1.9516	0.5249	0.3005	2.2437	0.2980	0.2380	2.2860	0.2721	0.1648
	2	2.4675	0.5689	0.3775	2.3869	0.3035	0.2463	2.3739	0.2901	0.1874
	3	2.4713	0.5942	0.3950	2.4379	0.3320	0.2574	2.3720	0.3290	0.2180
80[80%]	1	1.9551	0.3786	0.2374	2.1735	0.2400	0.1994	2.2574	0.1742	0.1347
	2	2.4599	0.3981	0.2561	2.2343	0.2682	0.2148	2.2761	0.1803	0.1400
	3	2.4507	0.5039	0.2872	2.2981	0.2743	0.2239	2.3070	0.2120	0.1550
					$T = 0.8$					
50[40%]	1	2.0806	0.6566	0.5212	1.9913	0.4462	0.3654	1.9759	0.4241	0.3445
	2	2.6568	0.6972	0.5742	2.1571	0.5111	0.4285	2.0291	0.4785	0.4012
	3	2.6314	0.7408	0.6051	2.0785	0.5416	0.4751	2.0086	0.5064	0.4241
50[80%]	1	2.0809	0.6147	0.4238	2.2741	0.3580	0.2615	2.2668	0.3218	0.2209
	2	2.4936	0.6233	0.4844	2.4441	0.3825	0.2816	2.3630	0.3433	0.2422
	3	2.4919	0.6381	0.5038	2.4925	0.4134	0.3097	2.3608	0.3875	0.2864
80[40%]	1	2.1086	0.4872	0.2828	2.1983	0.2793	0.2335	2.2602	0.2369	0.1543
	2	2.5160	0.5413	0.3096	2.3770	0.2943	0.2353	2.3762	0.2770	0.1689
	3	2.5044	0.5795	0.3426	2.4644	0.3257	0.2397	2.3879	0.3030	0.1945
80[80%]	1	2.2081	0.3530	0.2283	2.1534	0.2142	0.1929	2.2131	0.1586	0.1255
	2	2.4885	0.3833	0.2456	2.2624	0.2409	0.2115	2.2839	0.1691	0.1346
	3	2.4838	0.4400	0.2786	2.2631	0.2681	0.2194	2.2930	0.2066	0.1411

Table 5: The interval evaluations of ρ

n[FP%]	Scheme	95% ACI		95% HPD[P1]		95% HPD[P2]	
				$T = 0.4$			
50[40%]	1	1.830	0.906	0.473	0.929	0.265	0.943
	2	1.633	0.913	0.445	0.936	0.254	0.945
	3	1.543	0.917	0.423	0.940	0.246	0.949
50[80%]	1	1.358	0.920	0.363	0.943	0.243	0.952
	2	1.180	0.923	0.348	0.946	0.234	0.956
	3	0.986	0.925	0.327	0.948	0.223	0.958
80[40%]	1	0.803	0.929	0.302	0.952	0.214	0.959
	2	0.724	0.932	0.283	0.955	0.202	0.962
	3	0.686	0.937	0.258	0.960	0.198	0.966
80[80%]	1	0.630	0.940	0.236	0.964	0.179	0.969
	2	0.587	0.944	0.210	0.968	0.171	0.974
	3	0.529	0.947	0.201	0.971	0.156	0.977
				$T = 0.8$			
50[40%]	1	1.726	0.915	0.460	0.931	0.250	0.945
	2	1.533	0.922	0.434	0.938	0.246	0.947
	3	1.277	0.926	0.415	0.942	0.235	0.951
50[80%]	1	1.089	0.929	0.359	0.945	0.230	0.954
	2	0.982	0.932	0.341	0.948	0.224	0.957
	3	0.882	0.934	0.314	0.950	0.212	0.959
80[40%]	1	0.783	0.938	0.287	0.954	0.205	0.961
	2	0.678	0.941	0.259	0.957	0.197	0.963
	3	0.612	0.946	0.233	0.962	0.170	0.967
80[80%]	1	0.542	0.949	0.212	0.965	0.168	0.971
	2	0.519	0.953	0.202	0.970	0.162	0.975
	3	0.462	0.956	0.184	0.973	0.150	0.978

Table 6: The interval evaluations of τ

n[FP%]	Scheme	95% ACI		95% HPD[P1]		95% HPD[P2]	
				$T = 0.4$			
50[40%]	1	1.543	0.907	0.973	0.911	0.788	0.918
	2	1.638	0.903	1.098	0.908	0.812	0.915

(Continued)

Table 6 (continued)

n[FP%]	Scheme	95% ACI		95% HPD[P1]		95% HPD[P2]	
	3	1.743	0.889	1.359	0.903	0.854	0.910
50[80%]	1	1.347	0.916	0.670	0.928	0.644	0.931
	2	1.387	0.914	0.733	0.923	0.682	0.928
	3	1.413	0.911	0.835	0.917	0.729	0.924
80[40%]	1	1.236	0.926	0.493	0.938	0.465	0.941
	2	1.283	0.923	0.513	0.935	0.472	0.939
	3	1.307	0.920	0.562	0.932	0.491	0.937
80[80%]	1	1.072	0.935	0.353	0.949	0.326	0.951
	2	1.179	0.933	0.391	0.946	0.364	0.949
	3	1.200	0.930	0.437	0.941	0.414	0.945
				$T = 0.8$			
50[40%]	1	1.538	0.912	0.845	0.914	0.725	0.919
	2	1.573	0.908	0.913	0.911	0.748	0.916
	3	1.642	0.905	0.984	0.909	0.783	0.914
50[80%]	1	1.271	0.922	0.624	0.931	0.593	0.933
	2	1.328	0.918	0.683	0.928	0.607	0.931
	3	1.388	0.915	0.803	0.920	0.635	0.926
80[40%]	1	1.114	0.931	0.452	0.940	0.417	0.942
	2	1.170	0.928	0.499	0.936	0.428	0.941
	3	1.229	0.926	0.536	0.934	0.432	0.939
80[80%]	1	1.032	0.938	0.346	0.951	0.291	0.954
	2	1.096	0.937	0.385	0.947	0.326	0.951
	3	1.107	0.934	0.412	0.943	0.378	0.948

Table 7: The interval evaluations of $R(t)$

n[FP%]	Scheme	95% ACI		95% HPD[P1]		95% HPD[P2]	
				$T = 0.4$			
50[40%]	1	0.258	0.937	0.225	0.941	0.216	0.945
	2	0.226	0.940	0.211	0.944	0.195	0.948
	3	0.215	0.942	0.195	0.946	0.187	0.950
50[80%]	1	0.194	0.945	0.188	0.949	0.174	0.953
	2	0.191	0.946	0.187	0.950	0.172	0.954
	3	0.188	0.948	0.179	0.952	0.164	0.956
80[40%]	1	0.174	0.950	0.166	0.954	0.152	0.958
	2	0.168	0.952	0.156	0.956	0.138	0.960
	3	0.161	0.955	0.147	0.959	0.124	0.963

(Continued)

Table 7 (continued)

n[FP%]	Scheme	95% ACI		95% HPD[P1]		95% HPD[P2]	
80[80%]	1	0.153	0.958	0.141	0.962	0.114	0.966
	2	0.143	0.960	0.137	0.964	0.105	0.968
	3	0.139	0.962	0.127	0.966	0.098	0.970
				$T = 0.8$			
50[40%]	1	0.253	0.939	0.216	0.942	0.193	0.946
	2	0.220	0.941	0.208	0.944	0.187	0.949
	3	0.209	0.943	0.191	0.946	0.183	0.951
50[80%]	1	0.192	0.947	0.186	0.950	0.164	0.954
	2	0.189	0.949	0.182	0.952	0.154	0.957
	3	0.180	0.950	0.174	0.953	0.148	0.958
80[40%]	1	0.171	0.952	0.162	0.955	0.140	0.960
	2	0.165	0.953	0.152	0.956	0.136	0.961
	3	0.156	0.957	0.138	0.960	0.121	0.966
80[80%]	1	0.148	0.960	0.125	0.964	0.108	0.969
	2	0.135	0.961	0.114	0.966	0.101	0.971
	3	0.125	0.964	0.109	0.968	0.091	0.973

Table 8: The interval evaluations of $h(t)$

n[FP%]	Scheme	95% ACI		95% HPD[P1]		95% HPD[P2]	
				$T = 0.4$			
50[40%]	1	2.419	0.874	1.133	0.903	0.920	0.919
	2	2.694	0.870	1.203	0.897	0.944	0.915
	3	2.805	0.865	1.362	0.892	0.975	0.912
50[80%]	1	1.982	0.884	1.066	0.912	0.761	0.929
	2	2.087	0.882	1.088	0.908	0.800	0.926
	3	2.187	0.879	1.118	0.905	0.874	0.923
80[40%]	1	1.675	0.896	0.928	0.922	0.587	0.941
	2	1.752	0.892	0.967	0.919	0.599	0.938
	3	1.813	0.887	1.032	0.914	0.642	0.932
80[80%]	1	1.434	0.908	0.875	0.931	0.519	0.948
	2	1.485	0.904	0.900	0.928	0.547	0.945
	3	1.543	0.900	0.914	0.926	0.575	0.943

(Continued)

Table 8 (continued)

n[FP%]	Scheme	95% ACI		95% HPD[P1]		95% HPD[P2]	
				$T = 0.8$			
50[40%]	1	2.219	0.883	1.127	0.906	0.699	0.931
	2	2.488	0.877	1.190	0.900	0.748	0.925
	3	2.595	0.872	1.359	0.895	0.785	0.921
50[80%]	1	1.875	0.891	1.004	0.914	0.581	0.943
	2	1.980	0.889	1.051	0.912	0.611	0.939
	3	2.081	0.886	1.112	0.909	0.646	0.936
80[40%]	1	1.548	0.903	0.917	0.926	0.463	0.953
	2	1.653	0.899	0.948	0.922	0.471	0.951
	3	1.731	0.895	0.988	0.918	0.480	0.947
80[80%]	1	1.408	0.913	0.837	0.936	0.407	0.961
	2	1.473	0.910	0.876	0.933	0.420	0.959
	3	1.503	0.906	0.879	0.929	0.456	0.955

4.2 Simulation Discussions

This part addresses the assessment of the recommended inferential techniques. Based on the lowest RMSE, MAB, and AIL values as well as the highest CP values, we provide the following observations from Tables 1–8:

- All calculated point (or interval) estimates of ρ, τ, $R(t)$, or $h(t)$ behave satisfactorily.
- As n grows, all offered calculation findings become well. Identical observation is noted when $\sum_{j=1}^{m} S_i$ (or $n-m$) decreases.
- As T grows, the RMSEs, MABs, and AILs for the acquired estimates of all unknown subjects decrease while their CPs increase.
- The estimated CP values of ρ, τ, $R(t)$, or $h(t)$ are close to the preassigned 95% nominal level.
- Given that P2's variance is less than P1's, all Bayes outcomes based on P2 are better when compared to P1.
- Comparing the proposed estimation techniques, the derived point and interval estimators from the Bayes' paradigm provide more information than those produced using the likelihood paradigm.
- Comparing the proposed censoring patterns, estimates of τ and $h(t)$ behaved well with censoring [1],"both parameters ρ and $R(t)$ behaved well with censoring [3]."
- As a summary, for any practitioner dealing with an A-PT2C plan, we recommend using a Bayesian framework to estimate parameters or time reliability indices for the life of a GTL distribution.

5 Optimum Censoring

Today, due to the development of powerful statistical computing methods, optimal censoring is now applied in many fields, including engineering, economics, and medical research. Finding the best PT2C pattern to choose a sample means figuring out the best process among all the options that gives us the greatest amount of parameter knowledge of interest. Finding the optimal PT2C filtering among all possible patterns is the practitioner's importance in the reliability environment. The issue of selecting the optimum (ideal) PT2C design has been investigated in the statistical literature for reliability trial practitioners; for example, see Ng et al. [28], Dey and Elshahhat [29], and Mohammed et al. [30] among others. In Table 9, four ideal criteria are provided.

Table 9: Four criteria of optimum PT2C

Criterion	Objective
$\mathcal{C}_1$	Maximize trace($\mathbf{I}_{2\times2}(\boldsymbol{\vartheta})$)
$\mathcal{C}_2$	Minimize trace($\mathbf{I}^{-1}_{2\times2}(\boldsymbol{\vartheta})$)
$\mathcal{C}_3$	Minimize det($\mathbf{I}^{-1}_{2\times2}(\boldsymbol{\vartheta})$)
$\mathcal{C}_4$	Minimize $\widehat{var}(\log(\widehat{\Sigma}_\beta))$, $0 < \beta < 1$

To specify the criteria, $\mathcal{C}_1$ aims to maximize the estimated main diagonal elements of the observed FI matrix. Criteria $\mathcal{C}_i$, $i = 2, 3$, focus on minimizing the trace and determinant, respectively, of the estimated VC matrix. Meanwhile, criterion $\mathcal{C}_4$ seeks to minimize the variance of the logarithm of MLE for the γth quantile, denoted as $\widehat{var}(\log(\widehat{\Sigma}_\gamma))$, as follows:

$$\log(\widehat{\Sigma}_\gamma) = \frac{1}{\tau}\log\left(1-\sqrt{1-\gamma^{\frac{1}{\rho}}}\right),\ 0<\gamma<1,$$

where the delta technique is reconsidered here to get $\widehat{var}(\log(\widehat{\Sigma}_\gamma))$. To find the optimum PT2C, the experimenter should pick the design that has the highest value of $\mathcal{C}_1$ and the smallest values $\mathcal{C}_i$, $i = 2, 3, 4$.

6 Data Applications

This part presents two examples, using data from veterinary medicine and engineering, to show how the suggested methods can be utilized in real life.

6.1 Veterinary Medicine

From the veterinary medicine field, we shall analyze a data set representing the total milk production (TMP) at first birth of 107 cows from the SINDI race in Carnaúba farm, Agropecuária Manoel Dantas Ltda (AMDL), located in Taperoá City, Brazil. Following Cordeiro and dos Santos [31], in Table 10, the TMP data set is reported.

To determine if the GTL distribution is a suitable model for the TMP data, the Kolmogorov–Smirnov (KS) statistic (with its p-value) is found using the MLEs (along with their standard errors (Std.Es)) of ρ and τ. Based on Table 10, the KS(p-value), ρ, and τ fitted MLE values are, respectively, 2.3769(1.4704), 0.9125(0.3803), and 0.0984(0.251). As the predicted p-value exceeds the designated significance 5% level, we may conclude that the GTL model provides a substantial match to the TMP data. Fig. 4 shows the contour for the log-likelihood of ρ and τ. Additionally, we present three plots to visualize the fit result graphically: (i) estimated/empirical reliability, (ii) estimated/empirical scaled total-time-on-test (TTT) transform, and (iii) contour. Consequently, Fig. 4a demonstrates that the fitted-reliability line accurately reflected the empirical-reliability line, Fig. 4b points to an increasing failure rate in the TMP data, and Fig. 4c demonstrates the existence and uniqueness of the MLEs $\breve{\rho}$ and $\breve{\tau}$.

Table 10: The TMP data for cows from the SINDI race in Brazil

0.0168	0.0609	0.0650	0.0671	0.0776	0.0854	0.1131	0.1167	0.1479	0.1525
0.1546	0.2160	0.2303	0.2356	0.2361	0.2605	0.2681	0.2747	0.3134	0.3175
0.3188	0.3259	0.3323	0.3383	0.3406	0.3413	0.3480	0.3598	0.3627	0.3635
0.3751	0.3821	0.3891	0.3906	0.3945	0.4049	0.4111	0.4143	0.4151	0.4260
0.4332	0.4365	0.4371	0.4438	0.4470	0.4517	0.4530	0.4553	0.4564	0.4576
0.4612	0.4675	0.4694	0.4741	0.4752	0.4800	0.4823	0.4990	0.5113	0.5140
0.5150	0.5232	0.5285	0.5349	0.5350	0.5394	0.5447	0.5481	0.5483	0.5529
0.5553	0.5627	0.5629	0.5707	0.5744	0.5770	0.5853	0.5878	0.5912	0.5941
0.6012	0.6058	0.6114	0.6174	0.6196	0.6220	0.6465	0.6488	0.6707	0.6750
0.6768	0.6789	0.6844	0.6860	0.6891	0.6907	0.6927	0.7131	0.7261	0.7290
0.7471	0.7629	0.7687	0.7804	0.8147	0.8492	0.8781			

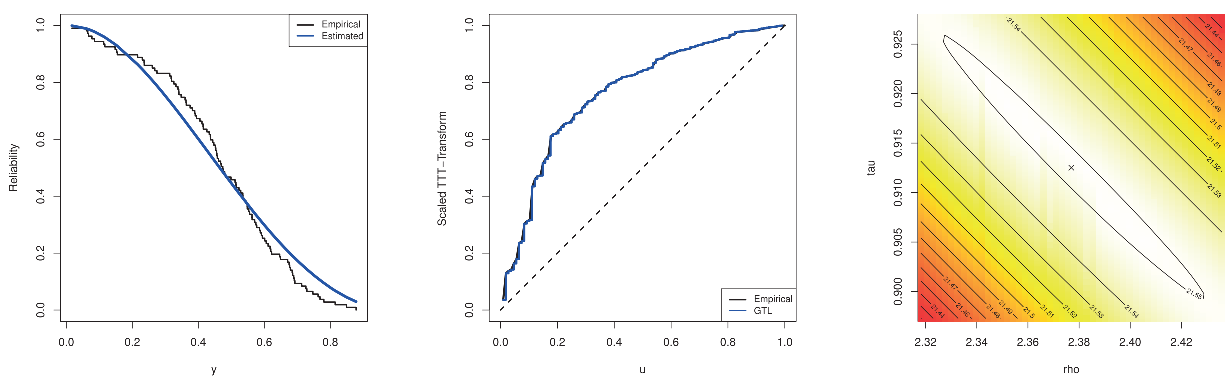

(a) (b) (c)

Figure 4: Plots of reliability (a), scaled TTT transform (b), and contour (c) from TMP data

Utilizing $m = 57$, several A-PT2C samples are generated from the whole TMP data depending on different T and $\mathbf{S}$ choices; refer to Table 11. Both the maximum likelihood and Bayes approaches of ρ, τ, $R(t)$, and $h(t)$ (at $t = 0.25$) yielded acquired point calculations (with their Std.Es) and 95% interval calculations (with their interval widths (IWs)) for each $\mathcal{S}i$ data for $i = 1, 2, 3$; see Table 12.

Since the prior information about ρ and τ from TMP data is not available, we consider the improper gamma priors to update MCMC iterations of ρ and τ, i.e., we set 0.0001 for $\alpha_i, \lambda_i,\ i = 1, 2$. Taking $\mathcal{V} = 40{,}000$ and $\mathcal{V}^{\circ} = 10{,}000$, all offered Bayes estimators as well as their 95% HPD intervals are evaluated. It is noted, from Table 12, that the point (or interval) estimates obtained from the likelihood setup are quite close to those obtained from the Bayes setup. To assess the existence and uniqueness of $\breve{\rho}$ and $\breve{\tau}$, the profile log-likelihoods are displayed in Fig. 5. It shows that the calculated estimates of $\breve{\rho}$ or $\breve{\tau}$, based on $\mathcal{S}i,\ i = 1, 2, 3$, exist and are unique. It also supports the same estimation values provided in Table 12.

Table 11: Three A-PT2C samples from TMP data

Sample	Censoring	$T(k)$	S_m^*	Data
$\mathcal{S}1$	$(10^5, 0^{52})$	0.70(2)	30	0.0168, 0.0650, 0.0776, 0.0854, 0.1167, 0.1479, 0.1525, 0.2303, 0.2356, 0.2605, 0.2681, 0.3175, 0.3259, 0.3323, 0.3383, 0.3406, 0.3413, 0.3480, 0.3598, 0.3627, 0.3635, 0.3751, 0.3821, 0.3906, 0.3945, 0.4049, 0.4111, 0.4143, 0.4260, 0.4332, 0.4365, 0.4371, 0.4470, 0.4517, 0.4530, 0.4553, 0.4564, 0.4576, 0.4612, 0.4675, 0.4694, 0.4741, 0.4800, 0.4823, 0.4990, 0.5113, 0.5140, 0.5150, 0.5232, 0.5285, 0.5349, 0.5350, 0.5394, 0.5447, 0.5481, 0.5483, 0.5529
$\mathcal{S}2$	$(0^{26}, 10^5, 0^{26})$	0.37(29)	20	0.0168, 0.0609, 0.0650, 0.0671, 0.0776, 0.0854, 0.1131, 0.1167, 0.1479, 0.1525, 0.1546, 0.2160, 0.2303, 0.2356, 0.2361, 0.2605, 0.2681, 0.2747, 0.3134, 0.3175, 0.3188, 0.3259, 0.3323, 0.3383, 0.3406, 0.3413, 0.3480, 0.3627, 0.3635, 0.3821, 0.3945, 0.4049, 0.4111, 0.4143, 0.4151, 0.4260, 0.4365, 0.4371, 0.4438, 0.4530, 0.4576, 0.4612, 0.4741, 0.4800, 0.4823, 0.4990, 0.5113, 0.5140, 0.5285, 0.5349, 0.5350, 0.5394, 0.5447, 0.5529, 0.5707, 0.5744, 0.5878
$\mathcal{S}3$	$(0^{52}, 10^5)$	0.52(56)	10	0.0168, 0.0609, 0.0650, 0.0671, 0.0776, 0.0854, 0.1131, 0.1167, 0.1479, 0.1525, 0.1546, 0.2160, 0.2303, 0.2356, 0.2361, 0.2605, 0.2681, 0.2747, 0.3134, 0.3175, 0.3188, 0.3259, 0.3323, 0.3383, 0.3406, 0.3413, 0.3480, 0.3598, 0.3627, 0.3635, 0.3751, 0.3821, 0.3891, 0.3906, 0.3945, 0.4049, 0.4111, 0.4143, 0.4151, 0.4260, 0.4332, 0.4365, 0.4371, 0.4438, 0.4470, 0.4517, 0.4530, 0.4553, 0.4564, 0.4576, 0.4612, 0.4675, 0.4694, 0.4823, 0.4990, 0.5140, 0.5394

Table 12: Estimates of ρ, τ, $R(t)$, and $h(t)$ from TMP data

Sample	Par.	MLE		MCMC		95% ACI			95% HPD		
		Est.	Std.E	Est.	Std.E	Lower	Upper	IW	Lower	Upper	IW
$\mathcal{S}1$	ρ	1.7681	1.2496	1.7592	0.1377	0.0000	4.2173	4.2173	1.4872	2.0209	0.5337
	τ	1.2163	0.6039	1.2201	0.0919	0.0327	2.4000	2.3673	1.0428	1.4019	0.3591
	$R(0.25)$	0.8545	0.0299	0.8510	0.0264	0.7959	0.9131	0.1172	0.8019	0.9032	0.1013
	$h(0.25)$	1.3152	0.2023	1.3308	0.1659	0.9186	1.7118	0.7931	1.0049	1.6495	0.6446
$\mathcal{S}2$	ρ	0.9686	0.6513	0.9712	0.1023	0.0000	2.2451	2.2451	0.7767	1.1745	0.3978
	τ	1.7949	0.9174	1.7919	0.1276	0.0000	3.5930	3.5930	1.5452	2.0436	0.4983
	$R(0.25)$	0.8313	0.0295	0.8278	0.0266	0.7734	0.8892	0.1158	0.7781	0.8800	0.1019
	$h(0.25)$	1.3499	0.1921	1.3647	0.1411	0.9734	1.7263	0.7529	1.0916	1.6363	0.5447
$\mathcal{S}3$	ρ	0.8849	0.6044	0.8884	0.0956	0.0000	2.0695	2.0695	0.7060	1.0777	0.3717
	τ	1.9215	1.0054	1.9163	0.1321	0.0000	3.8920	3.8920	1.6567	2.1729	0.5162
	$R(0.25)$	0.8305	0.0294	0.8270	0.0268	0.7729	0.8882	0.1153	0.7749	0.8782	0.1033
	$h(0.25)$	1.3376	0.1871	1.3525	0.1390	0.9709	1.7043	0.7335	1.0809	1.6195	0.5385

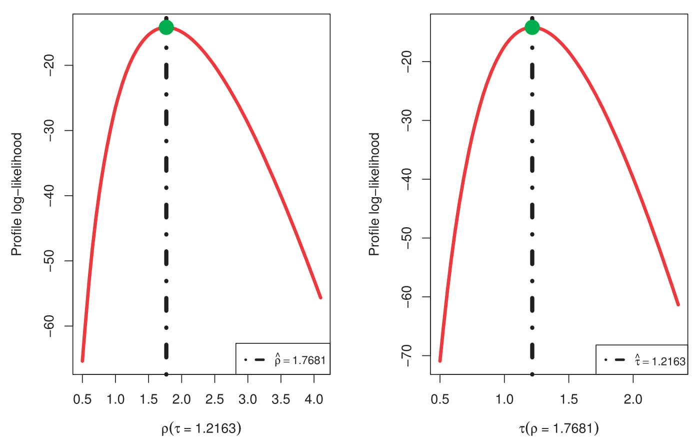

(a) Sample $\mathcal{S}1$

Figure 5: (Continued)

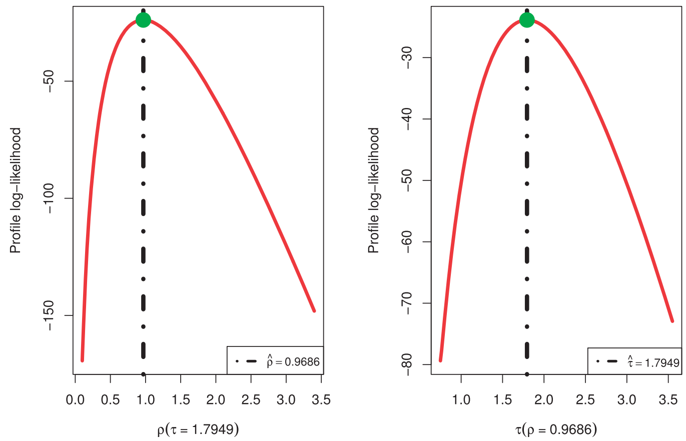

(b) Sample $\mathcal{S}2$

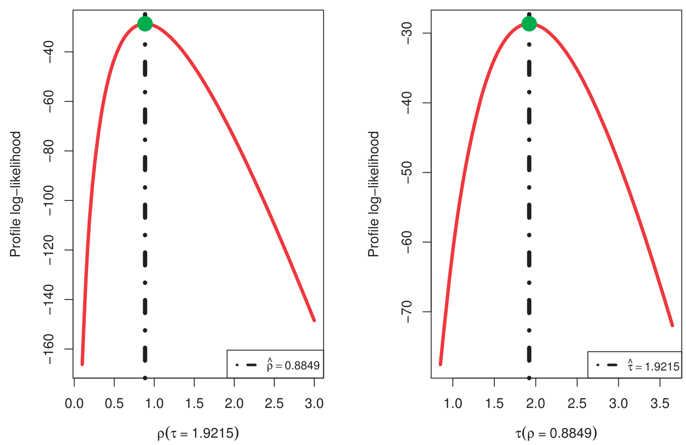

(c) Sample $\mathcal{S}3$

Figure 5: The log-likelihood curves of ρ and τ from TMP data

From Sample $\mathcal{S}_1$ (as an example), to see the convergence of the remaining 30,000 Markovian samples of ρ, τ, $R(t)$, and $h(t)$ from TMP data, trace and density diagrams are plotted in Fig. 6. It indicates that the estimated marginal estimates of μ, γ, and $h(t)$ are fairly symmetric, while those of $R(t)$ are negatively skewed. Additionally, it indicates that the burn-in period is precisely calibrated to remove the effects of the initial assumptions and achieve thorough mixing of the simulated samples.

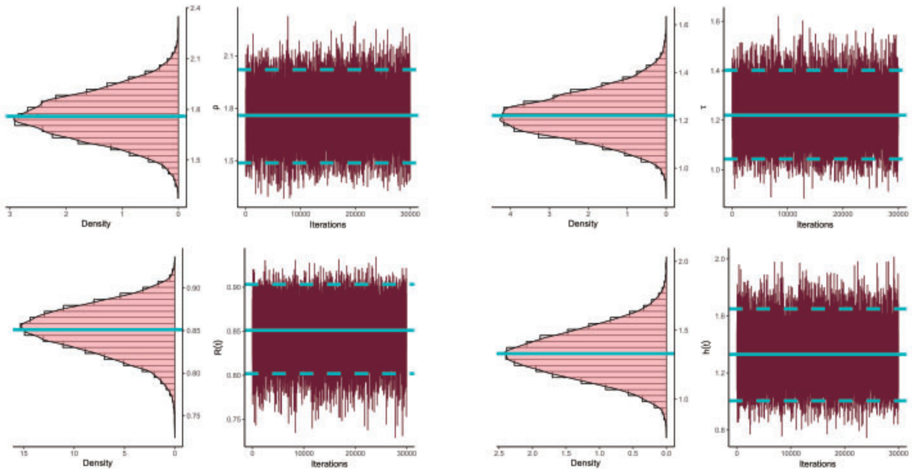

(a) Sample $\mathcal{S}1$

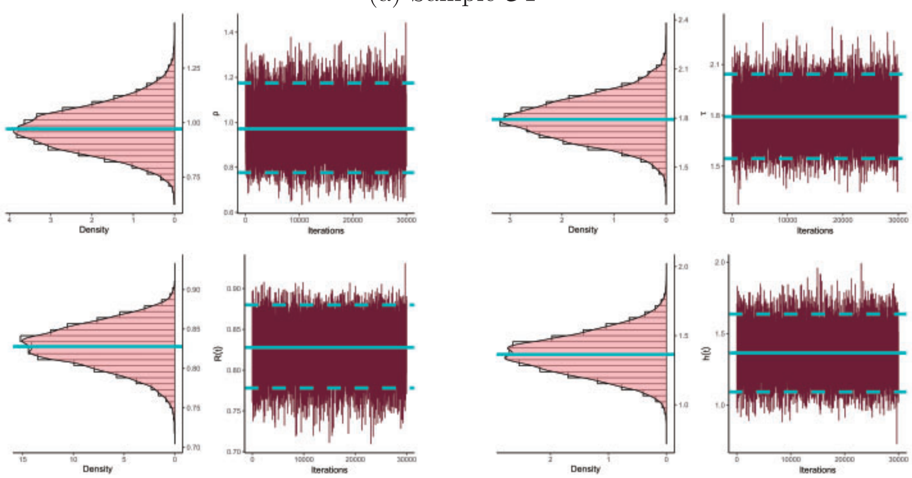

(b) Sample $\mathcal{S}2$

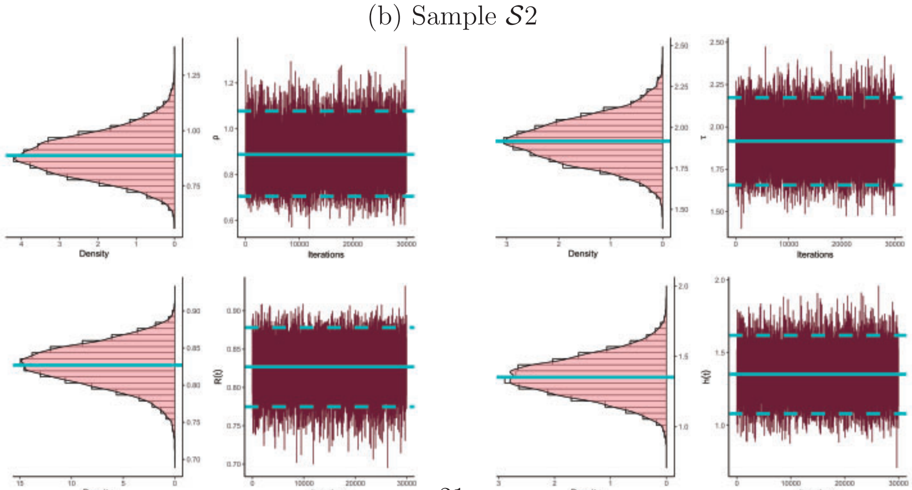

21

(c) Sample $\mathcal{S}3$

Figure 6: Trace (right) and Density (right) plots of ρ, τ, $R(t)$, and $h(t)$ from TMP data

Additionally, a number of statistics are calculated based on $\bar{\mathcal{V}} = 30{,}000$ MCMC outcomes of ρ, τ, $R(t)$, and $h(t)$; see Table 13. These statistics include mean, median, mode, first-quartile (Q_1), third-quartile (Q_3), standard deviation (Std.D.), and skewness (Sk.). Additionally, it confirms the results shown in Fig. 6 and presented in Table 12.

Table 13: Statistics of ρ, τ, $R(t)$, and $h(t)$ from TMP data

Sample	Par.	Mean	Mode	Q_1	Q_2	Q_3	Std.D.	Sk.
$\mathcal{S}1$	ρ	1.75915	1.99930	1.66415	1.75624	1.85263	0.13745	0.06641
	τ	1.22014	1.12604	1.15610	1.21759	1.28031	0.09185	0.18957
	$R(0.25)$	0.85104	0.85869	0.83421	0.85229	0.86957	0.02620	−0.31430
	$h(0.25)$	1.33076	1.30809	1.21629	1.32801	1.44138	0.16516	0.13972
$\mathcal{S}2$	ρ	0.97124	1.01280	0.89972	0.96844	1.03857	0.10226	0.19262
	τ	1.79193	1.71029	1.70325	1.78953	1.87717	0.12755	0.11664
	$R(0.25)$	0.82779	0.82835	0.81085	0.82887	0.84640	0.02638	−0.25552
	$h(0.25)$	1.36474	1.33429	1.26675	1.36373	1.45787	0.14031	0.07253
$\mathcal{S}3$	ρ	0.88837	0.80276	0.82078	0.88503	0.95148	0.09555	0.21645
	τ	1.91629	1.78125	1.82423	1.91471	2.00543	0.13199	0.10174
	$R(0.25)$	0.82697	0.81319	0.80970	0.82802	0.84556	0.02659	−0.27780
	$h(0.25)$	1.35253	1.37859	1.25749	1.35106	1.44402	0.13815	0.07724

The suggested criteria $\mathcal{C}_i$ for $i = 1, 2, 3, 4$ are assessed using the MLEs $\check{\rho}$ and $\check{\tau}$; see Table 14. This is done to address the problem of choosing the best censoring technique from the TMP data, as discussed in Section 5. It demonstrates that the censoring employed in $\mathcal{S}1$ is the best based on $\mathcal{C}_4$, the censoring employed in $\mathcal{S}2$ is the best based on $\mathcal{C}_2$, and the censoring employed in $\mathcal{S}3$ is the best based on $\mathcal{C}_i$ for $i = 1, 3$ compared to everyone else.

Table 14: The beat PT2C from TMP data

Sample	$\mathcal{C}_1$	$\mathcal{C}_2$	$\mathcal{C}_3$	$\mathcal{C}_4$		
$\beta \rightarrow$				0.3	0.6	0.9
$\mathcal{S}1$	149.679	1.926308	0.012870	0.000768	0.000848	0.000482
$\mathcal{S}2$	165.642	1.265822	0.007642	0.000779	0.000970	0.000583
$\mathcal{S}3$	182.656	1.376162	0.007534	0.000774	0.000972	0.000595

6.2 *Engineering*

Polyester is a synthetic textile manufactured primarily from petroleum. This fabric represents one of the most widely used fabrics in the world, with thousands of diverse consumer and manufacturing uses. In this example, we provide an analysis of engineering data that represents the 30 polyester fiber tensile strength (PFTS) measurements; see Quesenberry and Hales [32]. In Table 15, the PFTS data set is listed.

Table 15: Thirty measurements of PFTS

0.023	0.032	0.054	0.069	0.081	0.094	0.105	0.127	0.148	0.169
0.188	0.216	0.255	0.277	0.311	0.361	0.376	0.395	0.432	0.463
0.481	0.519	0.529	0.567	0.642	0.674	0.752	0.823	0.887	0.926

From Table 15, the fitted results of $\check{\rho}$, $\check{\tau}$, and KS(p-value) are 0.4894(0.7559), 1.8948(2.3816), and 0.0718(0.994), respectively. It indicates that the GTL lifetime model fits the PFTS data set satisfactorily. Again, the same three fitted plots depicted in Fig. 4 are replotted based on the complete PFTS data; see Fig. 7. However, Fig. 7 supports the same fitting result and shows that the fitted findings of ρ and τ exist and are unique as well.

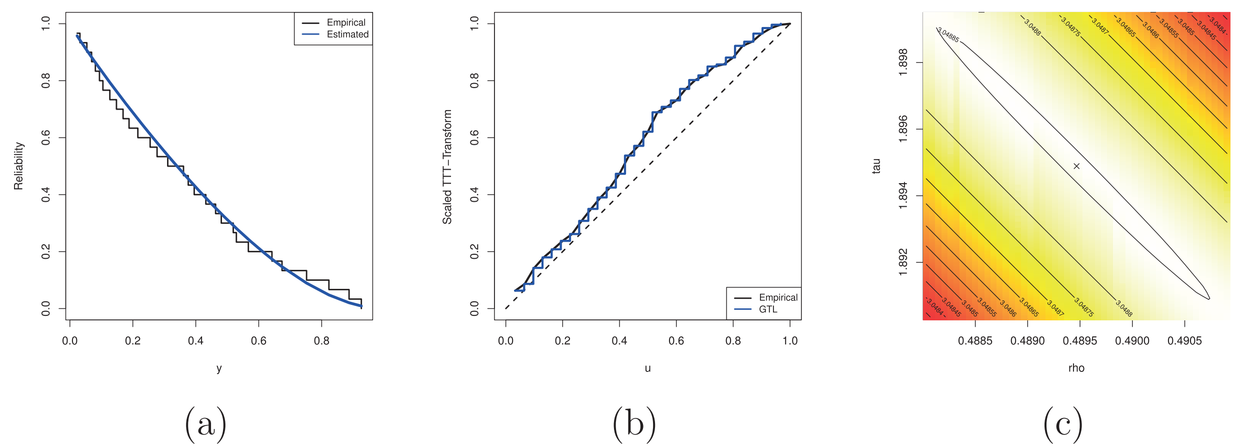

Figure 7: Plots of reliability (a), scaled TTT transform (b), and contour (c) from PFTS data

To assess the estimators of ρ, τ, $R(t)$, or $h(t)$, from Table 15, by assigning $m = 10$ and various selects of **S** and$T$, three A-PT2C samples are developed; see Table 16. For $\mathcal{S}$i, $i = 1, 2, 3$, the point and interval estimates of ρ, τ, $R(t)$, and $h(t)$ (at $t = 0.1$) are obtained; see Table 17. Just like the same settings discussed in Section 6.1, the Bayes evaluations are done. It is evident from Table 17 that both point and interval estimates developed by the Bayes approach perform similarly to those obtained from the likelihood approach. For $\mathcal{S}$i, $i = 1, 2, 3$, the profile log-likelihoods of ρ and τ are depicted in Fig. 8. It demonstrates that the obtained values of $\check{\rho}$ and $\check{\tau}$ exist and are unique, and it validates the estimated outcomes of ρ and τ shown in Table 17.

Again, using $\mathcal{S}$i, $i = 1, 2, 3$, two MCMC plots are displayed in Fig. 9. It reveals the good converging of the proposed M-H steps (proposed in Section 3) and the roughly symmetrical behavior of ρ and τ, despite $R(t)$ and $h(t)$ being positively and negatively skewed, respectively. Table 18 presents several statistics of ρ, τ, $R(t)$, and $h(t)$ as well as supporting the same results reported in Table 17.

Table 16: Three A-PT2C samples from PFTS data

Sample	Censoring	$T(k)$	S_m^*	Data
$\mathcal{S}1$	$(5^4, 0^6)$	0.25(1)	15	0.023, 0.054, 0.081, 0.094, 0.105, 0.127, 0.169, 0.216, 0.277, 0.311
$\mathcal{S}2$	$(0^3, 5^4, 0^3)$	0.95(5)	10	0.023, 0.032, 0.054, 0.069, 0.094, 0.148, 0.169, 0.188, 0.255, 0.311
$\mathcal{S}3$	$(0^6, 5^4)$	0.17(9)	5	0.023, 0.032, 0.054, 0.069, 0.081, 0.094, 0.105, 0.148, 0.188, 0.361

Table 17: Estimates of ρ, τ, $R(t)$, and $h(t)$ from PFTS data

Sample	Par.	MLE		MCMC		95% ACI			95% HPD		
		Est.	Std.E	Est.	Std.E	Lower	Upper	IW	Lower	Upper	IW
$\mathcal{S}1$	ρ	0.6182	1.3863	0.6177	0.1009	0.0000	3.3353	3.3353	0.4257	0.8140	0.3884
	τ	1.7835	3.2777	1.7770	0.1432	0.0000	8.2077	8.2077	1.5045	2.0689	0.5644
	$R(0.1)$	0.8794	0.0516	0.8700	0.0431	0.7782	0.9806	0.2024	0.7881	0.9454	0.1573
	$h(0.1)$	1.4994	0.5305	1.5554	0.3407	0.4595	2.5392	2.0797	0.9149	2.2078	1.2929
$\mathcal{S}2$	ρ	1.4324	2.9627	1.4233	0.1414	0.0000	7.2393	7.2393	1.1408	1.6956	0.5548
	τ	0.8536	1.3037	0.8538	0.1024	0.0000	3.4088	3.4088	0.6539	1.0534	0.3995
	$R(0.1)$	0.8543	0.0546	0.8449	0.0460	0.7473	0.9614	0.2141	0.7560	0.9278	0.1718
	$h(0.1)$	1.9275	0.7155	1.9921	0.4158	0.5252	3.3298	2.8046	1.1920	2.7901	1.5981
$\mathcal{S}3$	ρ	1.3243	3.0494	1.3151	0.1395	0.0000	7.3009	7.3009	1.0359	1.5819	0.5460
	τ	0.8773	1.5047	0.8778	0.1049	0.0000	3.8264	3.8264	0.6822	1.0902	0.4079
	$R(0.1)$	0.8424	0.0557	0.8328	0.0470	0.7332	0.9517	0.2185	0.7436	0.9195	0.1759
	$h(0.1)$	2.0184	0.7956	2.0822	0.4098	0.4590	3.5778	3.1188	1.3104	2.8854	1.5749

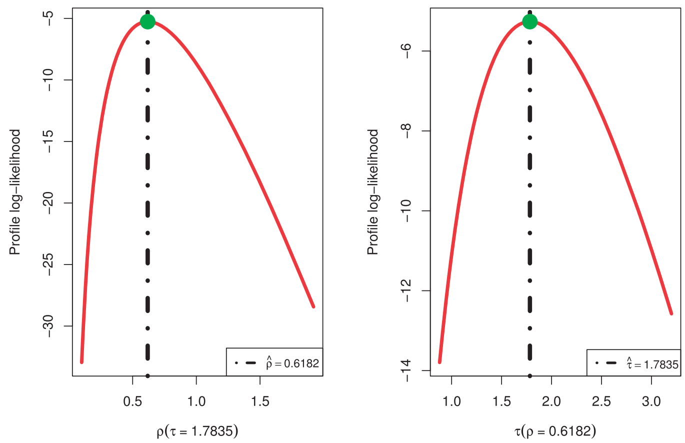

(a) Sample $\mathcal{S}1$

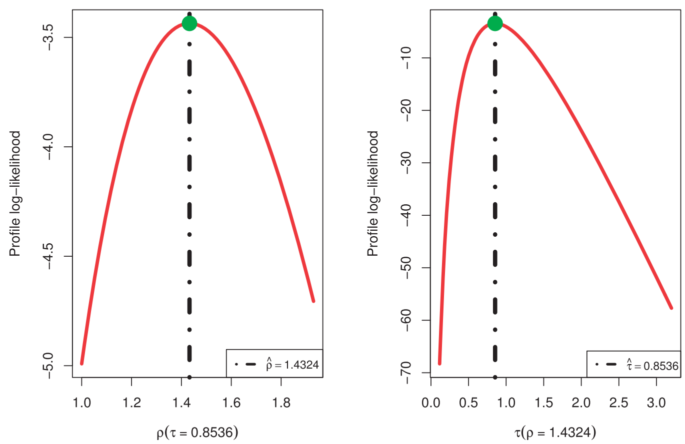

(b) Sample $\mathcal{S}2$

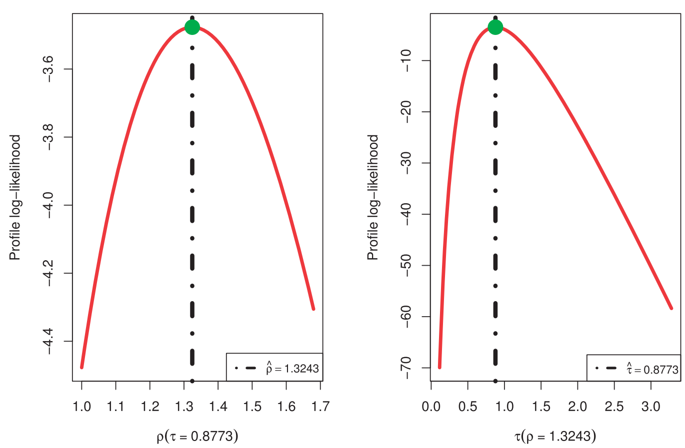

(c) Sample $\mathcal{S}3$

Figure 8: The log-likelihood curves of ρ and τ from PFTS data

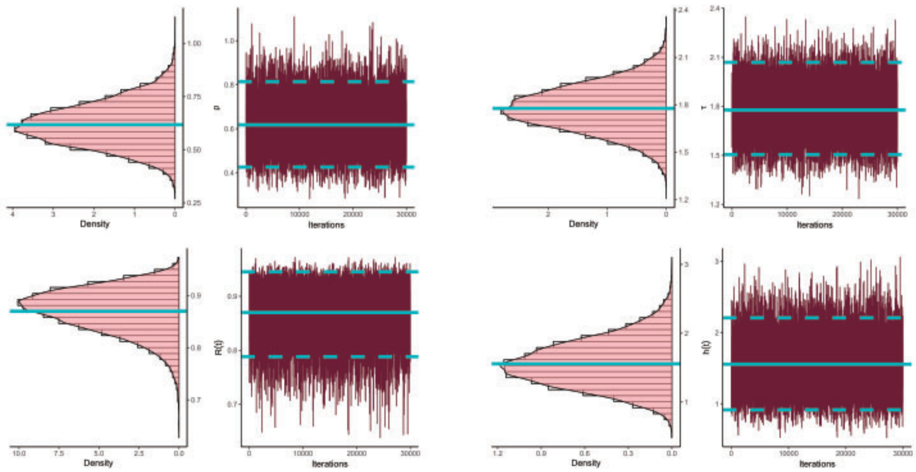

(a) Sample $\mathcal{S}1$

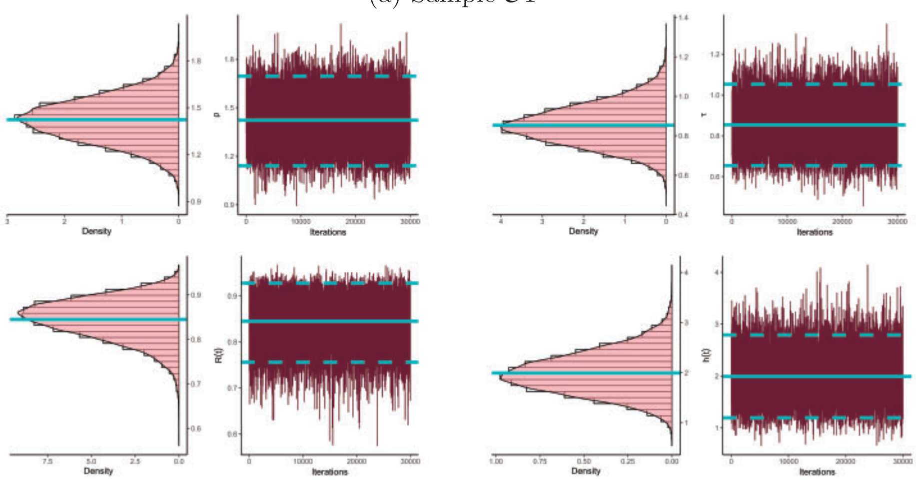

(b) Sample $\mathcal{S}2$

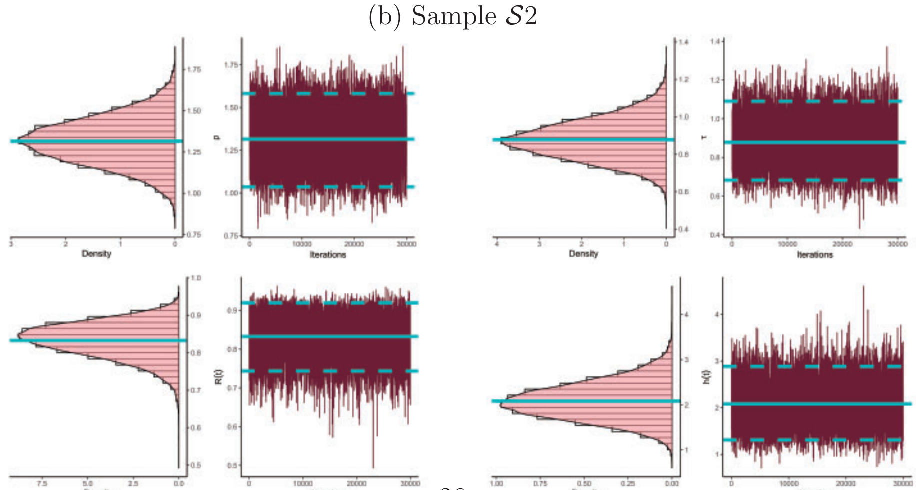

26

(c) Sample $\mathcal{S}3$

Figure 9: Trace (right) and Density (right) plots of ρ, τ, $R(t)$, and $h(t)$ from PFTS data

Table 18: Statistics of ρ, τ, $R(t)$, and $h(t)$ from PFTS data

Sample	Par.	Mean	Mode	Q_1	Q_2	Q_3	Std.D.	Sk.
$\mathcal{S}1$	ρ	0.61770	0.55567	0.54626	0.61410	0.68324	0.10085	0.23333
	τ	1.77700	1.43086	1.68064	1.77455	1.87338	0.14303	0.02452
	$R(0.1)$	0.87000	0.83783	0.84459	0.87502	0.90056	0.04206	−0.69915
	$h(0.1)$	1.55536	1.56118	1.31661	1.53885	1.77867	0.33612	0.28583
$\mathcal{S}2$	ρ	1.42326	1.36965	1.32652	1.42397	1.51753	0.14107	0.03401
	τ	0.85380	0.85375	0.78293	0.85059	0.92101	0.10244	0.20981
	$R(0.1)$	0.84491	0.84159	0.81737	0.84940	0.87721	0.04504	−0.58471
	$h(0.1)$	1.99205	2.03532	1.70505	1.97078	2.25759	0.41075	0.29420
$\mathcal{S}3$	ρ	1.31509	1.26149	1.21960	1.31532	1.40828	0.13916	0.04138
	τ	0.87777	0.87741	0.80457	0.87449	0.94682	0.10489	0.19727
	$R(0.1)$	0.83281	0.82809	0.80421	0.83685	0.86594	0.04603	−0.54457
	$h(0.1)$	2.08225	2.13468	1.79879	2.06332	2.34486	0.40475	0.26798

Table 19 points out that the censoring employed in $\mathcal{S}1$ is the most efficient based on $\mathcal{C}_3$, the censoring employed in $\mathcal{S}2$ is the optimal based on $\mathcal{C}_2$, and the censoring employed in $\mathcal{S}3$ is the best based on $\mathcal{C}_i$ for $i = 1, 4$ compared to the alternative. It is important to highlight that the outcomes shown in Tables 14 and 19 are consistent with the suggested censoring techniques outlined in Section 4.

Table 19: The beat PT2C from PFTS data

Sample	$\mathcal{C}_1$	$\mathcal{C}_2$	$\mathcal{C}_3$	$\mathcal{C}_4$		
$\beta \rightarrow$				0.3	0.6	0.9
$\mathcal{S}1$	79.5266	12.6651	0.13205	0.00384	0.01267	0.01223
$\mathcal{S}2$	79.7717	10.4773	0.15926	0.00274	0.01024	0.01190
$\mathcal{S}3$	79.3450	11.5628	0.14495	0.00271	0.00855	0.00923

As a summary, using total milk production at first calving of cows and full tensile strength data sets for polyester fibres, inferential results for the distribution parameters or reliability features of the generalized Topp-Leone model provide good behavior.

7 Conclusions

A recently developed statistical model, known as the extended Topp-Leone model, aims to provide insights into the functioning of medical, engineering, and chemistry processes. This model is good for data modeling with a bathtub or an increasing failure rate. Various statistical investigations from an A-PT2C have been conducted through the maximum likelihood and Bayesian inferential approach of the unknown model's parameters of life. Using the frequentist approach, we create an approximate confidence interval for each unknown quantity. Squared error loss has been suggested using it to producing Bayes estimates for the unknown parameters when we have a specific type of prior knowledge and gamma priors are available. It is important to note that while Bayes estimators can be described using MCMC methods, they generally cannot be derived in closed form. To assess the accuracy of the objective life parameters, Monte Carlo simulations revealed that the Bayesian approach outperforms traditional likelihood-based methods. Ideal censoring schemes were introduced, and various optimality criteria were analyzed. To evaluate the practical performance of the proposed methods, we examined two real-world datasets from veterinary medicine and engineering. Additionally, we extended several relevant works in the literature, some of which can be directly applied as special cases of our framework. The data analysis results demonstrate that the proposed model performs effectively under the given censored data conditions. In future research, the methodologies developed in this study could be extended to other reliability challenges, such as competing risks or accelerated life testing.

Acknowledgement: The authors would like to express thank to the Editor-in-Chief and anonymous referees for their constructive comments and suggestions. The authors express their gratitude to Princess Nourah bint Abdulrahman University Researchers Supporting Project number (PNURSP2025R175), Princess Nourah bint Abdulrahman University, Riyadh, Saudi Arabia.

Funding Statement: This research was funded by the Princess Nourah bint Abdulrahman University Researchers Supporting Project number (PNURSP2025R175), Princess Nourah bint Abdulrahman University, Riyadh, Saudi Arabia.

Author Contributions: The authors confirm contribution to the paper as follows: study conception and design: Heba S. Mohammed, Osama E. Abo-Kasem, Ahmed Elshahhat; data collection: Heba S. Mohammed; analysis and interpretation of results: Osama E. Abo-Kasem, Ahmed Elshahhat; draft manuscript preparation: Heba S. Mohammed, Osama E. Abo-Kasem, Ahmed Elshahhat. All authors reviewed the results and approved the final version of the manuscript.

Availability of Data and Materials: The data that support the findings of this study are available within the paper.

Ethics Approval: Not applicable.

Conflicts of Interest: The authors declare no conflicts of interest to report regarding the present study.

References

1. Topp CW, Leone FC. A family of J-shaped frequency functions. J Am Stat Assoc. 1955;50(269):209–19. doi:10.1080/01621459.1955.10501259.
2. Sangsanit Y, Bodhisuwan W. The Topp-Leone generator of distributions: properties and inferences. Songklanakarin J Sci Technol. 2016;38(5):537–48.
3. Alzaatreh A, Lee C, Famoye F. A new method for generating families of continuous distributions. Metron. 2013;71(1):63–79. doi:10.1007/s40300-013-0007-y.
4. Gupta RD, Kundu D. Introduction of shape/skewness parameter(s) in a probability distribution. J Probab Statist Sci. 2009;7(2):153–71.
5. Shekhawat K, Sharma VK. An extension of J-shaped distribution with application to tissue damage proportions in blood. Sankhya B. 2021;83(2):548–74. doi:10.1007/s13571-019-00218-6.
6. Ng HKT, Kundu D, Chan PS. Statistical analysis of exponential lifetimes under an adaptive type-II progressive censoring scheme. Naval Res Logist. 2009;56(8):687–98. doi:10.1002/nav.20371.

7. Liu S, Gui W. Estimating the parameters of the two-parameter Rayleigh distribution based on adaptive Type-II progressive hybrid censored data with competing risks. Mathematics. 2020;8(10):1783. doi:10.3390/math8101783.
8. Kohansal A, Bakouch HS. Estimation procedures for Kumaraswamy distribution parameters under adaptive Type-II hybrid progressive censoring. Commun Statist-Simulat Computat. 2021;50(12):4059–78. doi:10.1080/03610918.2019.1639734.
9. Elshahhat A, Nassar M. Bayesian survival analysis for adaptive Type-II progressive hybrid censored Hjorth data. Comput Stat. 2021;36(3):1965–90. doi:10.1007/s00180-021-01065-8.
10. Du Y, Gui W. Statistical inference of adaptive Type-II progressive hybrid censored data with dependent competing risks under bivariate exponential distribution. J Appl Stat. 2022;49(12):3120–40. doi:10.1080/02664763.2021.1937961.
11. Alotaibi R, Elshahhat A, Rezk H, Nassar M. Inferences for alpha power exponential distribution using adaptive progressively type-II hybrid censored data with applications. Symmetry. 2022;14(4):651. doi:10.3390/sym14040651.
12. Nassar M, Alotaibi R, Dey S. Estimation based on adaptive progressively censored under competing risks model with engineering applications. Mathem Prob Eng. 2022. doi:10.1155/2022/6731230.
13. Elshahhat A, Nassar M. Analysis of adaptive Type-II progressively hybrid censoring with binomial removals. J Stat Comput Simul. 2023;93(7):1077–103. doi:10.1080/00949655.2022.2127149.
14. Elshahhat A, Alotaibi R, Nassar M. Reliability and the engineering applications of the generalized half-normal model via an adaptive progressive hybrid censored mechanism. AIP Adv. 2023;13(11):115310. doi:10.1063/5.0175806.
15. Muhammed HZ, Almetwally EM. Bayesian and non-bayesian estimation for the shape parameters of new versions of bivariate inverse weibull distribution based on progressive type II censoring. Computat J Mathem Statist Sci. 2024;3(1):85–111. doi:10.21608/cjmss.2023.250678.1028.
16. El-Saeed AR, Abdellatif AD. Point and interval estimation of reliability and entropy for generalized exponential distribution under generalized type-II hybrid censoring scheme. Comput J Mathemat Statist Sci. 2025;4(1):96–138. doi:10.21608/cjmss.2024.327558.1078.
17. Henningsen A, Toomet O. maxLik: a package for maximum likelihood estimation in R. Comput Stat. 2011;26(3):443–58. doi:10.1007/s00180-010-0217-1.
18. Bayoud HA. Estimating the shape parameter of Topp-Leone distribution based on progressive type II censored samples. REVSTAT-Statist J. 2016;14(4):415–31. doi:10.57805/revstat.v14i4.196.
19. Feroze N, Aslam M, Khan IH, Khan MH. Bayesian reliability estimation for the Topp-Leone distribution under progressively type-II censored samples. Soft Comput. 2021;25(3):2131–52. doi:10.1007/s00500-020-05285-w.
20. İlhan USTA. Bayesian estimation for Topp-Leone distribution using progressively censored data and asymmetric loss functions. Sigma J Eng Nat Sci. 2022;40(1):9–26. doi:10.14744/sigma.2022.00002.
21. Feroze N, Aslam M. On Bayesian analysis of failure rate under Topp Leone distribution using complete and censored samples. Int J Math Comput Phys Electr Comput Eng. 2013;7(3):426–32.
22. Arora S, Mahajan KK, Kumari R. Bayes estimators for the reliability and hazard rate functions of Topp-Leone distribution using Type-II censored data. Communicat Statist-Simul Computat. 2021;50(8):2327–44. doi:10.1080/03610918.2019.1602646.
23. Wasserman L. All of statistics: a concise course in statistical inference. Berlin/Heidelberg, Germany: Springer Science and Business Media; 2013.
24. Gelman A, Carlin JB, Stern HS, Rubin DB. Bayesian data analysis. 2nd ed. Boca Raton, FL, USA: Chapman and Hall/CRC; 2004.
25. Chen MH, Shao QM. Monte Carlo estimation of Bayesian credible and HPD intervals. J Comput Graph Stat. 1999;8(1):69–92. doi:10.1080/10618600.1999.10474802.

26. Kundu D. Bayesian inference and life testing plan for the Weibull distribution in presence of progressive censoring. Technometrics. 2008;50(2):144–54. doi:10.1198/004017008000000217.
27. Plummer M, Best N, Cowles K, Vines K. Coda: convergence diagnosis and output analysis for MCMC. R News. 2006;6(1):7–11.
28. Ng HKT, Chan CS, Balakrishnan N. Optimal progressive censoring plans for the Weibull distribution. Technometrics. 2004;46(4):470–81. doi:10.1198/004017004000000482.
29. Dey S, Elshahhat A. Analysis of Wilson-Hilferty distribution under progressive type-II censoring. Qual Reliab Eng Int. 2022;38(7):3771–96. doi:10.1002/qre.3173.
30. Mohammed HS, Elshahhat A, Alotaibi R. Inferences of inverted Gompertz parameters from an adaptive type-II progressive hybrid censoring. Phys Scr. 2023;98(10):105222. doi:10.1088/1402-4896/acf5ad.
31. Cordeiro GM, dos Santos RB. The beta power distribution. Braz J Probab Stat. 2012;26(1):88–112. doi:10.1214/10-bjps124.
32. Quesenberry CP, Hales C. Concentration bands for uniformity plots. J Stat Comput Simul. 1980;11(1):41–53. doi:10.1080/00949658008810388.